[redacted]

CENTRAL RESEARCH LIBRARY
DOCUMENT COLLECTION

RPL 1/26/5

ORNL-1818
Chemistry-Separation Processes for Plutonium and Uranium

AEC RESEARCH AND DEVELOPMENT REPORT

cy. 4

MARTIN MARIETTA ENERGY SYSTEMS LIBRARIES
3 4456 0349801 6

PRODUCTS PRODUCED IN BATCH NEUTRON IRRADIATION OF THORIUM

A. T. Gresky
E. D. Arnold

CENTRAL RESEARCH LIBRARY
DOCUMENT COLLECTION
LIBRARY LOAN COPY
DO NOT TRANSFER TO ANOTHER PERSON
If you wish someone else to see this document, send in name with document and the library will arrange a loan.

OAK RIDGE NATIONAL LABORATORY
OPERATED BY
UNION CARBIDE NUCLEAR COMPANY
A Division of Union Carbide and Carbon Corporation
UCC
POST OFFICE BOX P · OAK RIDGE, TENNESSEE

[redacted]

[redacted]

ORNL-1818

Copy No. 4

Contract No. W-7405-eng-26

CHEMICAL TECHNOLOGY DIVISION

PRODUCTS PRODUCED IN BATCH NEUTRON IRRADIATION OF THORIUM

A. T. Gresky

E. D. Arnold

DECLASSIFIED

CLASSIFICATION CHANGED TO:

BY AUTHORITY OF: TID-1149

BY: D. Menzon 7/24/57

DATE ISSUED

OAK RIDGE NATIONAL LABORATORY
Operated by
UNION CARBIDE NUCLEAR COMPANY
A Division of Union Carbide and Carbon Corporation
Post Office Box P
Oak Ridge, Tennessee

[redacted]

[redacted]

MARTIN MARIETTA ENERGY SYSTEMS LIBRARIES

3 4456 0349801 6

ORNL-1818
Chemistry-Separation Processes
for Plutonium and Uranium
M-3679 (16th ed.)

INTERNAL DISTRIBUTION

1. C. E. Center
2. Biology Library
3. Health Physics Library
4-5. Central Research Library
6. Reactor Experimental Engineering Library
7-11. Laboratory Records Department
12. Laboratory Records, ORNL R.C.
13. A. M. Weinberg
14. L. B. Emlet (K-25)
15. J. P. Murray (Y-12)
16. J. A. Swartout
17. E. H. Taylor
18. E. D. Shipley
19-20. F. L. Culler
21. F. C. VonderLage
22. W. H. Jordan
23. C. P. Keim
24. J. H. Frye, Jr.
25. S. C. Lind
26. A. H. Snell
27. A. Hollaender
28. M. T. Kelley
29. K. Z. Morgan
30. T. A. Lincoln
31. R. S. Livingston
32. A. S. Householder
33. C. S. Harrill
34. C. E. Winters
35. D. W. Cardwell
36. E. M. King
37. W. K. Eister
38. F. R. Bruce
39. D. E. Ferguson
40. H. K. Jackson
41. H. E. Goeller
42. D. D. Cowen
43. R. A. Charpie
44. J. A. Lane
45. M. J. Skinner
46. R. E. Blanco
47. G. E. Boyd
48. W. E. Unger
49. R. R. Dickison
50. B. F. Bottenfield
51. A. C. Jealous
52. R. W. Stoughton
53. E. M. Shank
54. R. P. Wischow
55. E. D. Arnold
56. A. T. Gresky
57. S. Peterson
58. ORNL Document Reference Library, Y-12 Branch

EXTERNAL DISTRIBUTION

59. Alco Products, Inc.
60-65. Argonne National Laboratory
66. Armed Forces Special Weapons Project (Sandia)
67. Armed Forces Special Weapons Project, Washington
68-70. Atomic Energy Commission, Washington
71. Bettis Plant (WAPD)
72-74. Brookhaven National Laboratory
75. Bureau of Ships
76. Union Carbide Nuclear Company (C-31 Plant)
77-79. Union Carbide Nuclear Company (K-25 Plant)
80. Chicago Patent Group
81. Dow Chemical Company (Rocky Flats)
82-85. duPont Company, Augusta

86. duPont Company, Wilmington
87-94. General Electric Company, Richland
95. Goodyear Atomic Corporation
96. Hanford Operations Office
97. Iowa State College
98-100. Knolls Atomic Power Laboratory
101-102. Los Alamos Scientific Laboratory
103. Massachusetts Institute of Technology (Benedict)
104. Mound Laboratory
105. Naval Research Laboratory
106. New York Operations Office
107-108. North American Aviation, Inc.
109. Patent Branch, Washington
110-113. Phillips Petroleum Company (NRTS)
114-115. University of California Radiation Laboratory, Berkeley
116-117. University of California Radiation Laboratory, Livermore
118. Vitro Engineering Division
119. Division of Research and Medicine, AEC, ORO
120-184. Technical Information Service, Oak Ridge

[redacted]

CONTENTS

		Page
1.0	Abstract	1
2.0	Introduction	1
3.0	Plotted Data	1
4.0	Formation of U^{232} from Th^{232}	5
5.0	Calculations	30
6.0	Constants and Definition of Symbols	35
7.0	References	37

[redacted]

[redacted]

1.0 ABSTRACT

Calculated data and graphs describing the effects of batch thermal-neutron irradiation of thorium, the usual method of operation of heterogeneous reactors, are presented. The buildup and decay of U^{233}, Pa^{233}, other heavy isotopes, and fission products are considered on the basis of best available cross-section and fission-yield data. The effects of these irradiation products on the Thorex chemical separation process are indicated briefly.

2.0 INTRODUCTION

The purpose of the study reported here was to calculate the amounts of various products that would be produced by batch neutron irradiation of thorium in a heterogeneous reactor.* The information thus obtained would be used as a basis for determining the extent of irradiation that is both desirable and permissible and the decay time required for reasonable chemical processing schedules in the Thorex process plants. Data were calculated for fluxes of 10^{13}, 10^{14}, and 10^{15} $n/cm^2/sec$, based on nuclear reactions known to occur (Fig. 1) when Th^{232} is irradiated and on the estimated amounts of specific fission products (Fig. 2) formed in fission of U^{233}. The data were plotted in both summary and detailed form. Amounts of products remaining after various post-reactor decay times were also calculated and plotted. The products considered were U^{232}, U^{233}, U^{234}, U^{235}, U^{236}, U^{237}, Th^{233}, Th^{234}, Ru^{103}, Ru^{106}, and the Ba^{140}-La^{140} chain.

3.0 PLOTTED DATA

Figs. 3-8: Composite plots showing the amounts of various products formed as a function of irradiation time. Values are given for fluxes of 10^{13}, 10^{14}, and 10^{15} $n/cm^2/sec$. The data are tabulated in Tables 1-3.

* Similar calculations for continuous irradiation in a homogeneous reactor are given in ORNL-1817.[1]

[redacted]

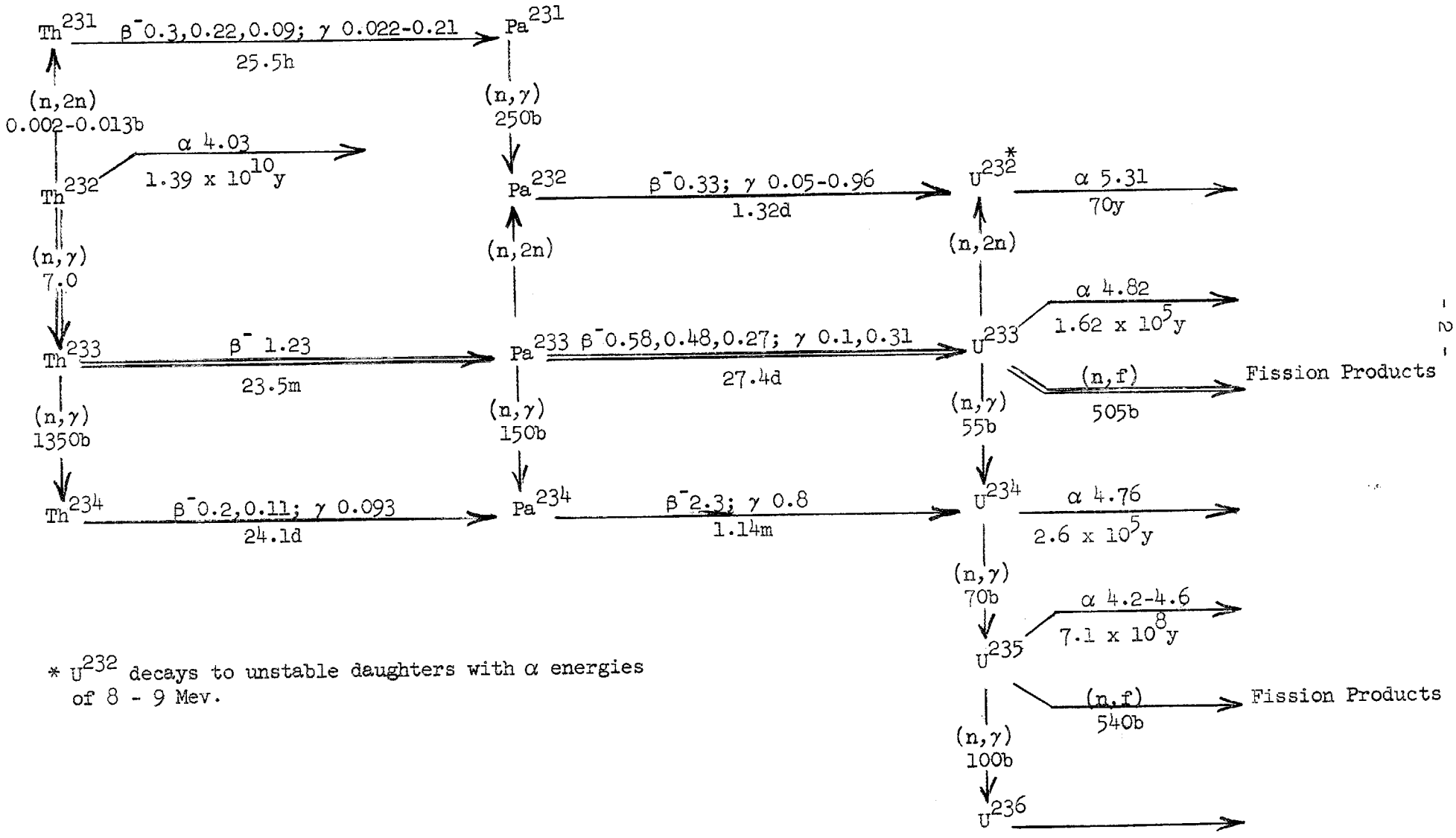

* U^{232} decays to unstable daughters with α energies of 8 - 9 Mev.

Fig. 1. NUCLEAR REACTIONS THAT OCCUR WHEN Th^{232} IS IRRADIATED WITH THERMAL NEUTRONS. CROSS-SECTION DATA WERE OBTAINED FROM REFERENCES 2, 3, AND 4.

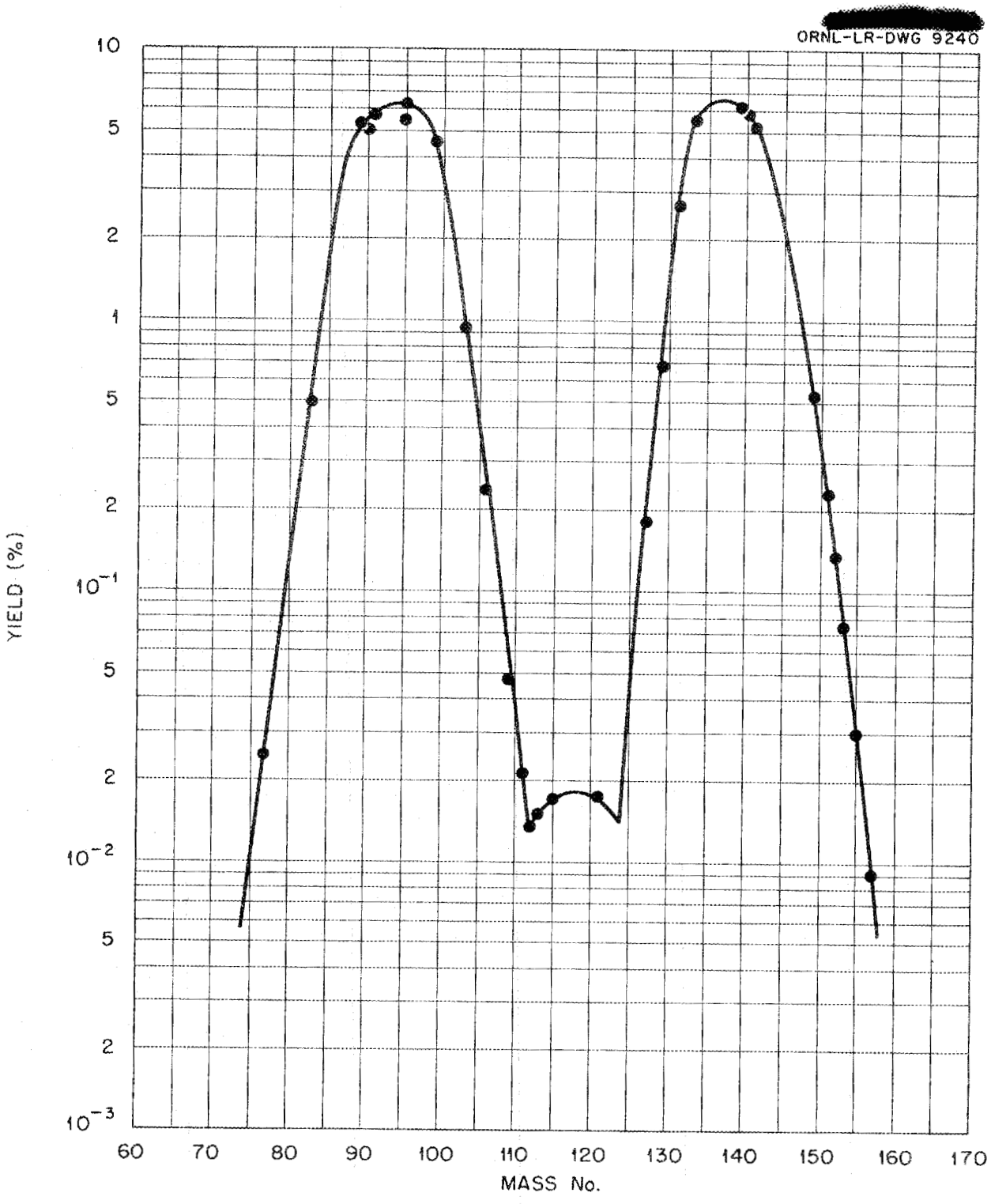

Fig. 2. U^{233} Fission Yield Curve.

Fig. 9: Plot showing production of isotopes of mass-233 as a function of flux and time.

Figs. 10 and 11: Plots showing the Pa^{233}/U^{233} concentration ratio as a function of flux and irradiation time and of flux and decay time after discharge, respectively. At time of discharge, following irradiation at a flux of 10^{15} n/cm^2/ sec, in material containing 3000 g of isotopes of mass-233 per ton of thorium, 92% of the 233 isotope would be Pa^{233}. Chemical processing (Thorex) of such material after a short decay time can be visualized as an expedient means of obtaining large quantities of isotopically pure U^{233}, which would be formed by decay of the Pa^{233} in the Thorex extraction column aqueous waste.

Figs. 12-14: Plots showing amount of U^{232} formed, the U^{232}/U^{233} α activity ratio as a function of irradiation time and flux, and the U^{232} and daughter activities as a function of decay time after discharge. U^{232} data are tabulated in Table 4. The U^{232} chain is known to contain members that emit 8- to 9-Mev α particles highly efficient in causing (α,n) reactions on light metals, e.g., carbon and boron, which may contaminate the final U^{233} metal product.[5,6] The α activity values plotted in Fig. 13 are those of U^{232} alone and do not include the activities of the five daughters, which grow in with a 1.9y half-life. The total α activity at equilibrium ($\sim$12.5y) would be approximately 6 times that of U^{232}. The cross-section values of 2-13 mb represent the characteristic spread of reported data, which are known to vary with reactor moderation and neutron energy distributions.

Figs. 15-17: Plots showing the amount of Th^{234} formed as a function of flux, the Th^{234} β activity as a function of g/t level, flux, and decay time, and the decay time required to reduce the Th^{234} β activity to $< 10^9$ d/m per kilogram of thorium. This value is considered the maximum β activity permissible for a thorium product destined for subsequent direct handling in metallurgical operations. It is readily observed that the Th^{234}/Th^{232} ratio increases roughly as the square of the flux; very long decay periods after discharge would therefore be imposed by irradiations at a flux of 10^{15} or even at the 10^{14} n/cm^2/sec proposed for the Thermal Breeder Reactor blanket.

Figs. 18-20: Plots showing Ru^{103} and Ru^{106} activities as a function of flux, g/t level, and decay time after discharge. If a ruthenium decontamination factor of 100 is assumed for the thorium product, it can be shown that the additional activity contributed by Ru^{103} is eliminated during the time required for the Th^{234} activity to decay. However, the ly Ru^{106} becomes limiting with fluxes of 10^{13} or 10^{14} $n/cm^2/sec$ at production levels of greater than 1000 g/t. The activity of Ru^{106} will in these cases then require a minimum ruthenium decontamination factor of 10^3 to reduce the total ruthenium activity below 10^9 d/m/kg Th^{232} even with the long period required for Th^{234} to decay. Ruthenium data are tabulated in Table 5.

The widely varying compositions of Thorex process feeds that may be visualized in long-range projections involving thorium irradiation may demand significant flexibility in processing philosophy.

4.0 FORMATION OF U^{232} FROM Th^{232}

It is generally agreed that U^{232} is produced in reactors chiefly by the reactions

$$Th^{232}(n,2n)Th^{231} \xrightarrow[25.5h]{\beta} Pa^{231}(n,\gamma)Pa^{232} \xrightarrow[1.32d]{\beta} U^{232} \xrightarrow[70y]{\alpha}$$

The (n,2n) reaction can occur only with neutrons with energy greater than the 5-6 Mev neutron binding energy. The relative amounts of (n,2n) reactions can vary with different reactors or even in different regions of the same reactor owing to the different extents of moderation. Because of the high energy necessary for reaction, only a small fraction of neutrons enter into (n,2n) reactions, and this small fraction decreases with increased moderation of the reactor.

The (n,2n) cross sections for reactor neutrons have been variously reported as 2-13 mb, although there have been some data indicating ~1 mb. In this report the range 2-13 mb was used to indicate the concentration and activity of U^{232}. Table 4 shows the effect of U^{232} concentration of the α activity of the total mass-233 produced, while Figs. 12 and 13 indicate the U^{232} concentrations and the U^{232}/U^{233} α activity ratios, respectively.

Table 1. Amounts of Products Produced by Neutron Irradiation of Thorium at Flux of 10^{13} n/cm^2/sec

Irradiation Time (days)	g of Isotope per kg of Th							
	Pa^{233}	U^{233}	$Pa^{233} + U^{233}$	U^{234}	U^{233} F.P.'s	Th^{234}	U^{235}	Th Burnup
5	0.0285	0.0017	0.0302	0.0548×10^{-4}	2.8×10^{-6}	7.78×10^{-7}		0.0304
10	0.0535	0.0070	0.0605	0.229×10^{-4}	2.22×10^{-5}	1.45×10^{-6}	8×10^{-9}	0.0607
20				0.841×10^{-4}	1.78×10^{-4}	2.56×10^{-6}	6.35×10^{-8}	0.1214
25	0.1122	0.0402	0.1524					
30				1.932×10^{-4}	6.01×10^{-4}	3.41×10^{-6}	2.15×10^{-7}	0.1821
40							5.11×10^{-7}	0.2428
50	0.171	0.133	0.304	4.260×10^{-4}	1.4×10^{-3}	4.32×10^{-6}	1×10^{-6}	0.3035
75	0.203	0.253	0.456					
80							2.2×10^{-6}	
100	0.219	0.392	0.611	1.250×10^{-3}	7.2×10^{-3}	5.56×10^{-6}	4.3×10^{-6}	0.607
150	0.2325	0.654	0.8865	2.232×10^{-3}	1.4×10^{-2}	5.84×10^{-6}	1.45×10^{-5}	
200				3.682×10^{-3}	2.65×10^{-2}	5.89×10^{-6}	3.44×10^{-5}	1.214
250	0.238	1.223	1.461	5.018×10^{-3}	4.64×10^{-2}	5.91×10^{-6}	6.70×10^{-5}	
300				6.565×10^{-3}	8.87×10^{-2}	5.91×10^{-6}	1.16×10^{-4}	1.821
350	0.238	1.745	1.983	8.132×10^{-3}	1.2×10^{-1}	5.91×10^{-6}	1.59×10^{-4}	
400	0.238			9.480×10^{-3}	1.52×10^{-1}	5.91×10^{-6}	2.37×10^{-4}	2.428
450	0.238	2.25	2.488	1.109×10^{-2}	1.84×10^{-1}	5.91×10^{-6}	3.39×10^{-4}	
500	0.238	2.505	2.743	1.299×10^{-2}	2.60×10^{-1}	5.91×10^{-6}	4.65×10^{-4}	3.035
550	0.238			1.470×10^{-2}	3.14×10^{-1}	5.91×10^{-6}	6.1×10^{-4}	
600	0.238	2.98	3.218	1.666×10^{-2}	3.80×10^{-1}	5.91×10^{-6}	8.0×10^{-4}	3.642
650	0.238	3.19	3.428	1.850×10^{-2}	4.45×10^{-1}	5.91×10^{-6}	1.0×10^{-3}	
700	0.238	3.41	3.748	2.048×10^{-2}	5.11×10^{-1}	5.91×10^{-6}	1.27×10^{-3}	4.249
750	0.238	3.64	3.878	2.243×10^{-2}	5.88×10^{-1}	5.91×10^{-6}		
800	0.238	3.83	4.068	2.450×10^{-2}	6.77×10^{-1}	5.91×10^{-6}		4.856
850	0.238	4.03	4.268			5.91×10^{-6}		
900	0.238	4.24	4.478	2.794×10^{-2}	8.53×10^{-1}	5.91×10^{-6}		5.463
1000	0.238	4.63	4.868	3.332×10^{-2}	1.04	5.91×10^{-6}		6.070

Table 2. Amounts of Products Produced by Neutron Irradiation of Thorium at Flux of 10^{14} n/cm^2/sec

Irradiation Time (days)	g of Isotope per kg of Th							
	Pa^{233}	U^{233}	$Pa^{233} + U^{233}$	U^{234}	U^{233} F.P.'s	Th^{234}	U^{235}	Th Burnup
2						3.31×10^{-5}		0.1214
3						4.55×10^{-5}		
4						6.30×10^{-5}		0.2428
5	0.284	0.022	0.306	0.00052	2.84×10^{-4}	7.78×10^{-5}		0.3035
10	0.531	0.084	0.615	0.0021	2.23×10^{-3}	1.45×10^{-4}	8×10^{-6}	0.607
20				0.014	1.78×10^{-2}	2.56×10^{-4}	6.35×10^{-5}	1.214
25	1.100	0.390	1.490					
30				0.033	2.61×10^{-2}	3.41×10^{-4}	2.20×10^{-4}	1.821
40							5.2×10^{-4}	2.428
50	1.675	1.174	2.849	0.083	9.45×10^{-2}	4.32×10^{-4}	1.0×10^{-3}	3.035
60							1.76×10^{-3}	3.642
70							2.80×10^{-3}	
75	1.965	2.155	4.120					
80							4.84×10^{-3}	4.856
90							6.39×10^{-3}	
100	2.110	3.14	5.250	0.277	5.55×10^{-1}	5.56×10^{-4}	7.75×10^{-3}	6.070
150	2.230	4.925	7.155	0.483	1.44	5.84×10^{-4}	1.52×10^{-2}	9.105
200				0.728	2.68	5.89×10^{-4}	2.71×10^{-2}	12.140
250				1.035	4.19	5.91×10^{-4}	4.55×10^{-2}	15.175
300				1.338	5.95	5.91×10^{-4}	6.67×10^{-2}	18.210
350				1.67	7.87	5.91×10^{-4}	9.26×10^{-2}	21.245
400				1.99	9.94	5.91×10^{-4}	1.19×10^{-1}	24.280
450				2.32	12.08	5.91×10^{-4}	1.48×10^{-1}	27.315
500				2.63	14.32	5.91×10^{-4}	1.77×10^{-1}	30.350

Table 3. Amounts of Products Produced by Neutron Irradiation of Thorium at Flux of 10^{15} n/cm^2/sec

Irradiation Time (days)	g of Isotope per kg of Th													
	Pa^{233}	U^{233}	$Pa^{233} + U^{233}$	U^{234}	U^{233} F.P.'s	Th^{234}	U^{235}	U^{235} F.P.'s	Total F.P.	U^{236} Chain	U^{236}	U^{237}	Np^{237} Chain	Total Th Burnup
1	0.606	0.002	0.608			1.63×10^{-3}	8×10^{-6}							0.607
2	1.183	0.06	1.243	0.0172	1.78×10^{-3}	3.31×10^{-3}	6.35×10^{-5}		1.78×10^{-3}					1.214
3	1.745	0.13	1.875	0.0206	6.02×10^{-3}	4.55×10^{-3}	2.15×10^{-4}		6.02×10^{-3}					1.821
4	2.27	0.16	2.43	0.0773	1.43×10^{-2}	6.30×10^{-3}	5.0×10^{-4}		1.43×10^{-2}					2.428
5	2.77	0.21	2.98	0.099	2.79×10^{-2}	7.78×10^{-3}	9.9×10^{-4}		2.79×10^{-2}					3.035
6	3.25	0.26	3.51				1.72×10^{-3}							3.642
7	3.73	0.31	4.04				2.73×10^{-3}							4.249
10	5.03	0.54	5.57	0.424	9.95×10^{-2}	1.45×10^{-2}	1.82×10^{-2}		9.95×10^{-2}					6.070
20				1.042	0.547	2.56×10^{-2}	1.61×10^{-2}		0.547					12.14
25	9.75	2.40	12.15											15.175
30				2.495	1.642	3.41×10^{-2}	2.05×10^{-1}	7.3×10^{-2}	1.72					18.210
40							2.82×10^{-1}	1.85×10^{-1}						24.280
50	13.50	5.25	18.75	5.636	5.303	4.32×10^{-2}	3.71×10^{-1}	3.35×10^{-1}	5.64					30.350
60								5.7×10^{-1}		1.05×10^{-1}	1.05×10^{-1}	7.4×10^{-4}	1.7×10^{-3}	36.420
75	15.0	6.88	21.88				7.97×10^{-1}	1.05		1.85×10^{-1}	1.85×10^{-1}			45.525
80														48.560
90								1.65		3.05×10^{-1}	2.93×10^{-1}	3.64×10^{-3}	8.36×10^{-3}	54.630
100	15.50	7.68	23.18	13.88	19.876	5.56×10^{-2}	1.21	2.20	22.08	4.05×10^{-1}	3.90×10^{-1}			60.700
150	15.85	8.25	24.10	20.675	37.235	5.84×10^{-2}	2.01	5.96	43.20	1.1	1.02	2.43×10^{-2}	5.7×10^{-2}	91.050
200				25.837	55.073	5.89×10^{-2}	2.65	11.3	66.37	2.0	1.82	8.6×10^{-2}	1.42×10^{-1}	121.400
250				29.650	73.046	5.91×10^{-2}	3.12	17.0	90.05	3.3	2.87	1.32×10^{-1}	3.20×10^{-1}	151.75
300				32.484	91.020	5.91×10^{-2}	3.47	25.9	116.9	4.75	3.97	2.38×10^{-1}	5.38×10^{-1}	182.100
350				34.594	109.707	5.91×10^{-2}	3.67	33.7	143.4	6.30	5.05	3.80×10^{-1}	8.70×10^{-1}	212.450
400				36.137	126.97	5.91×10^{-2}	3.92	42.5	169.5	8.0	6.10	5.70×10^{-1}	1.30	242.800
450				37.319	144.95	5.91×10^{-2}	4.06	51.6	196.6	9.9	7.25	7.90×10^{-1}	1.80	273.15
500				38.151	162.92	5.91×10^{-2}	4.17	60.7	223.6					303.50

[redacted]
ORNL-LR-DWG 9241

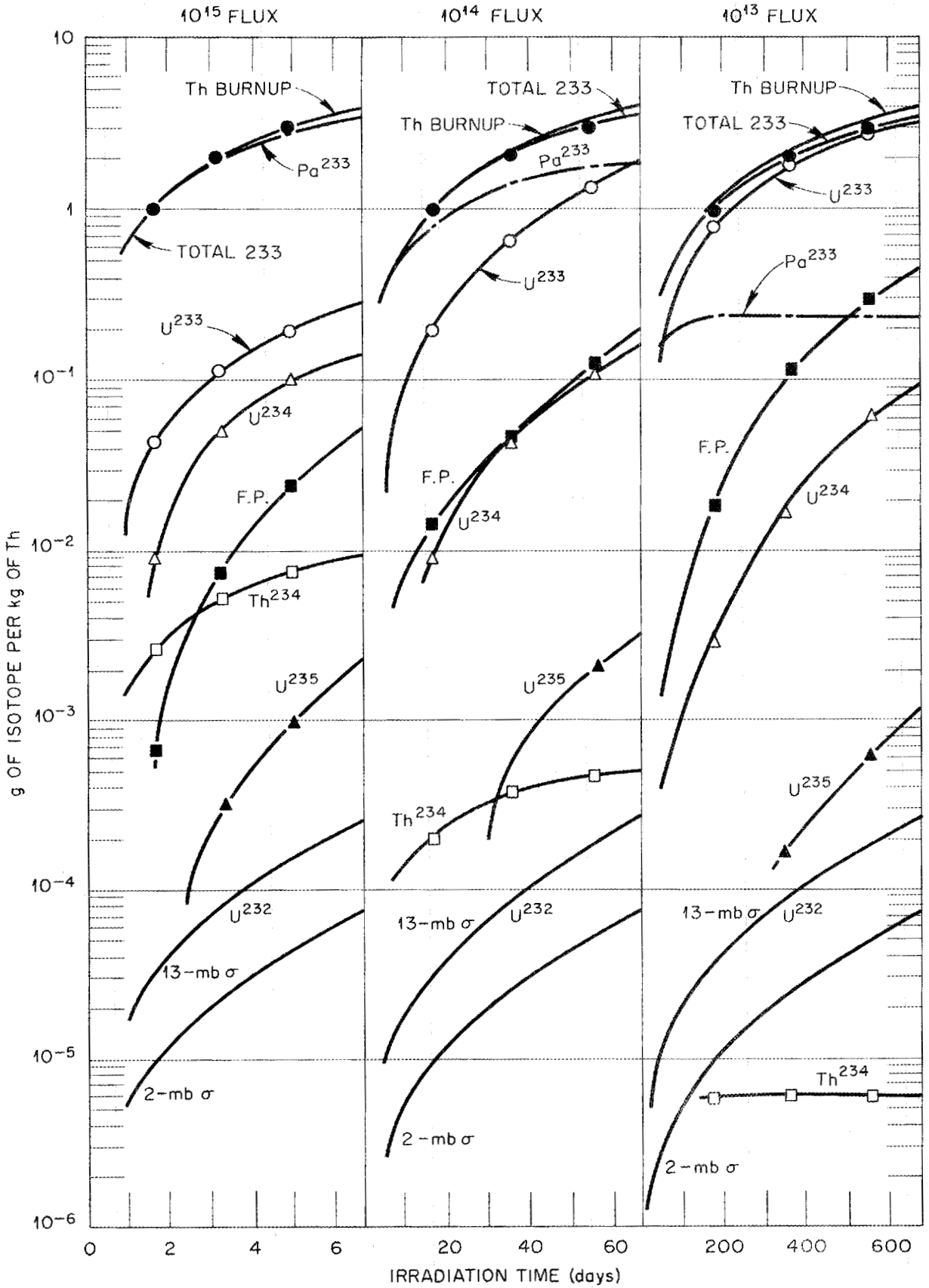

Fig. 3. Summary of Th^{232} Neutron Irradiation Data. Details are given in Figs. 4 through 6.

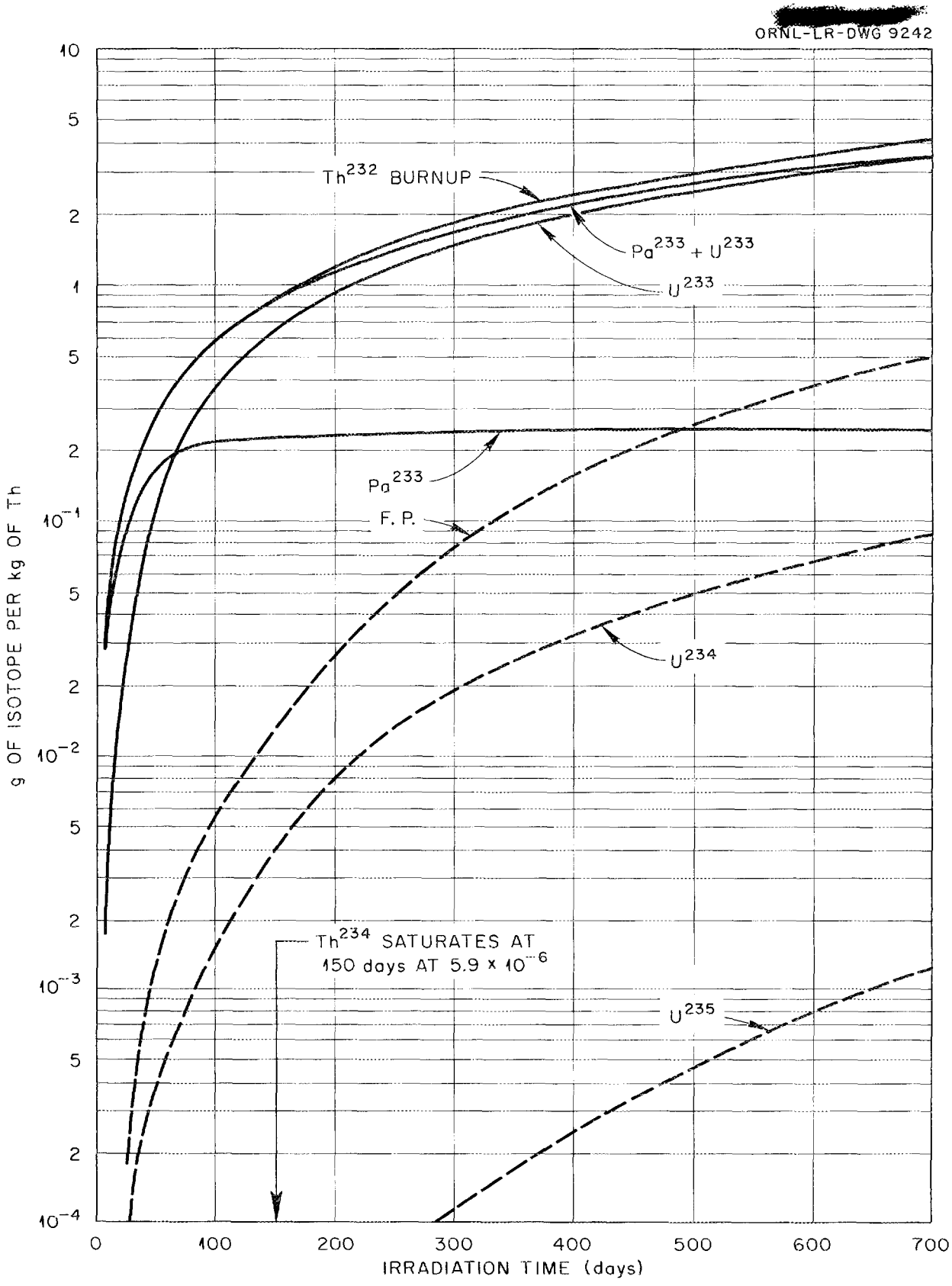

Fig. 4. Details of Products Produced by Neutron Irradiation of Th^{232} at Flux of 10^{13} neutrons/cm^2 • sec.

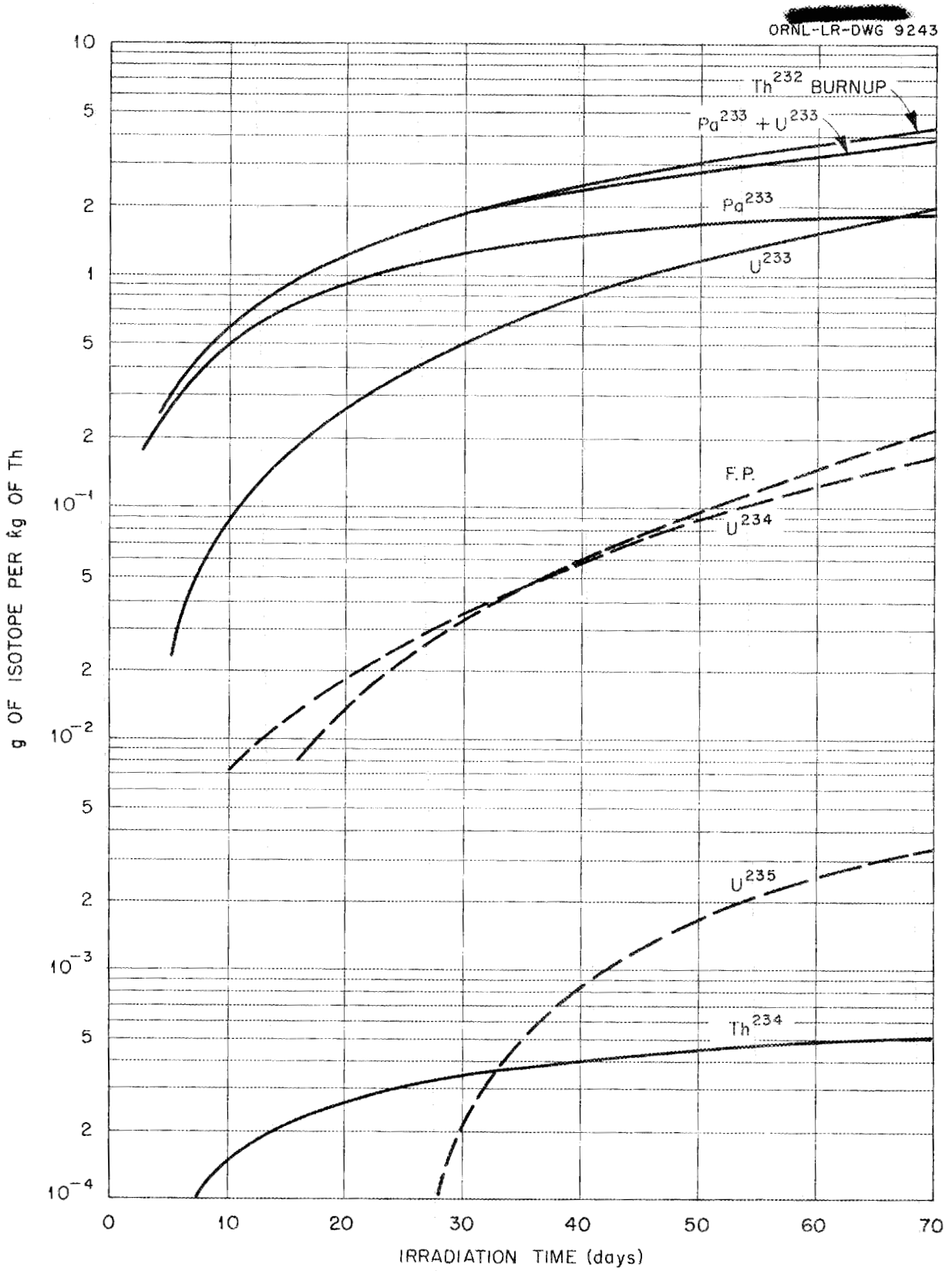

Fig. 5. Details of Products Produced by Neutron Irradiation (Short-Term) of Th^{232} at Flux of 10^{14} neutrons/cm^2·sec.

[redacted]

ORNL-LR-DWG 9244

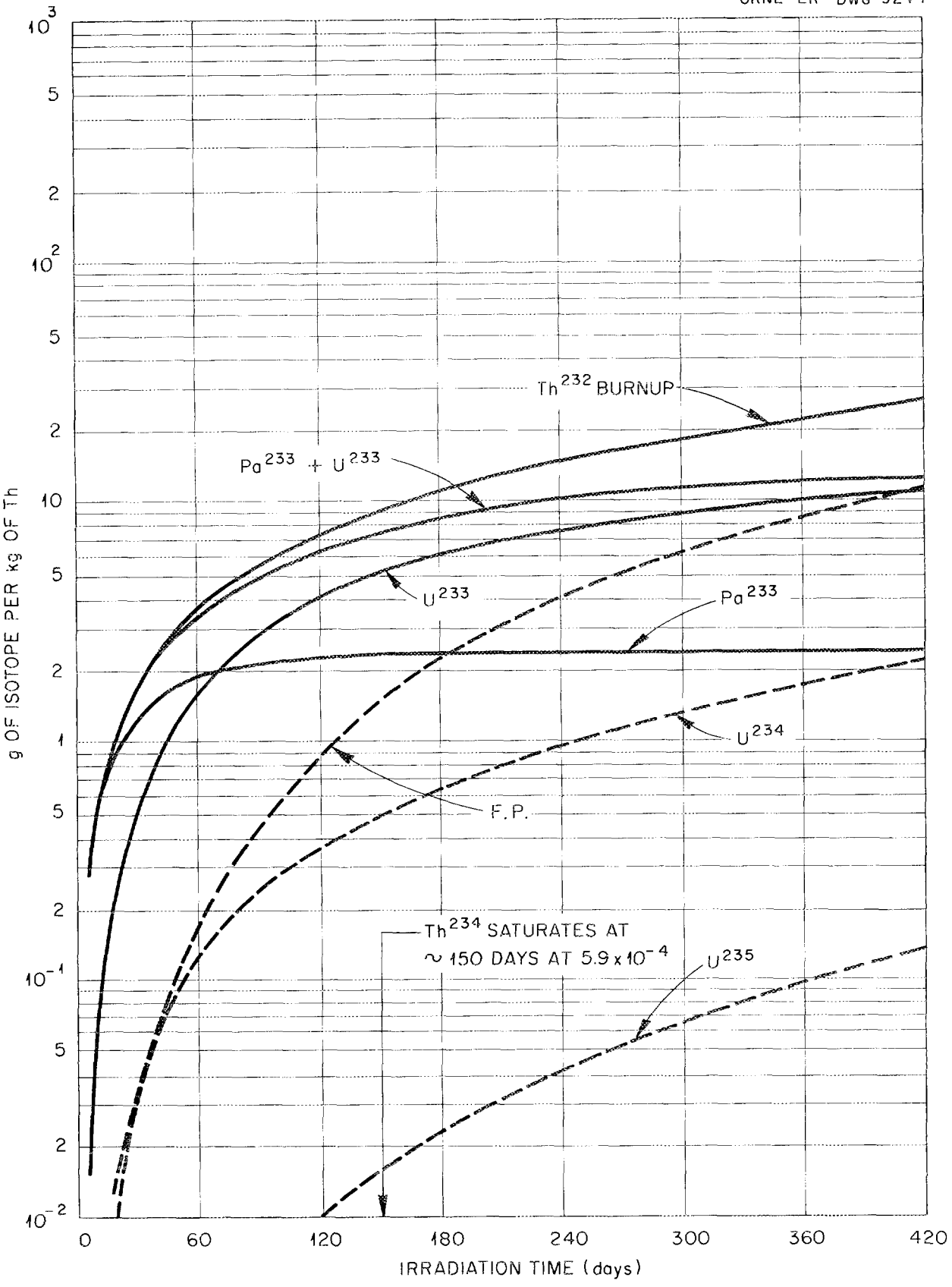

Fig. 6. Details of Products Produced by Neutron Irradiation (Long Term) of Th^{232} at Flux of 10^{14} neutrons/$cm^2 \cdot sec$.

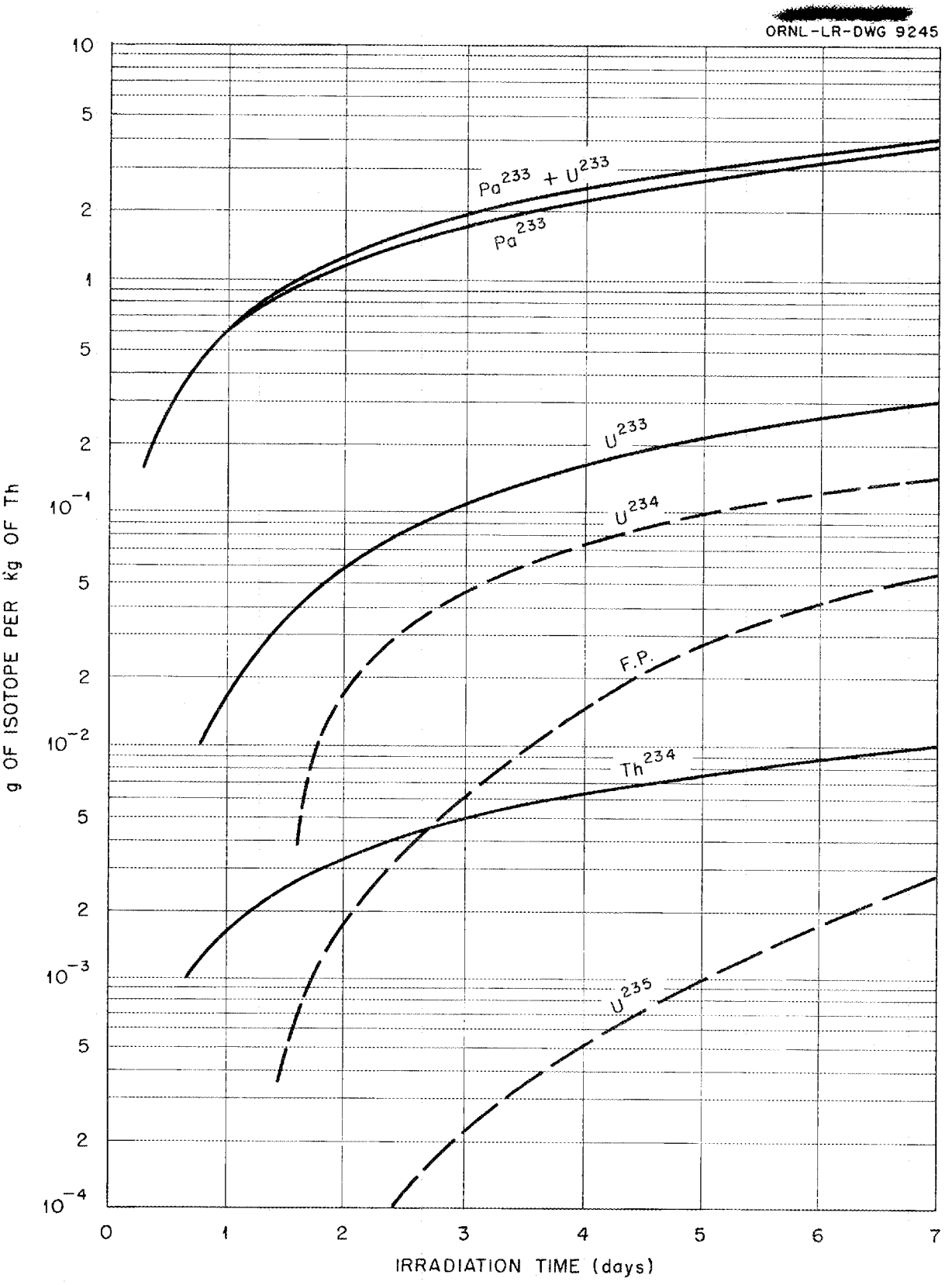

Fig. 7. Details of Products Produced by Neutron Irradiation (Short-Term) of Th^{232} at Flux of 10^{15} neutrons/cm^2 · sec.

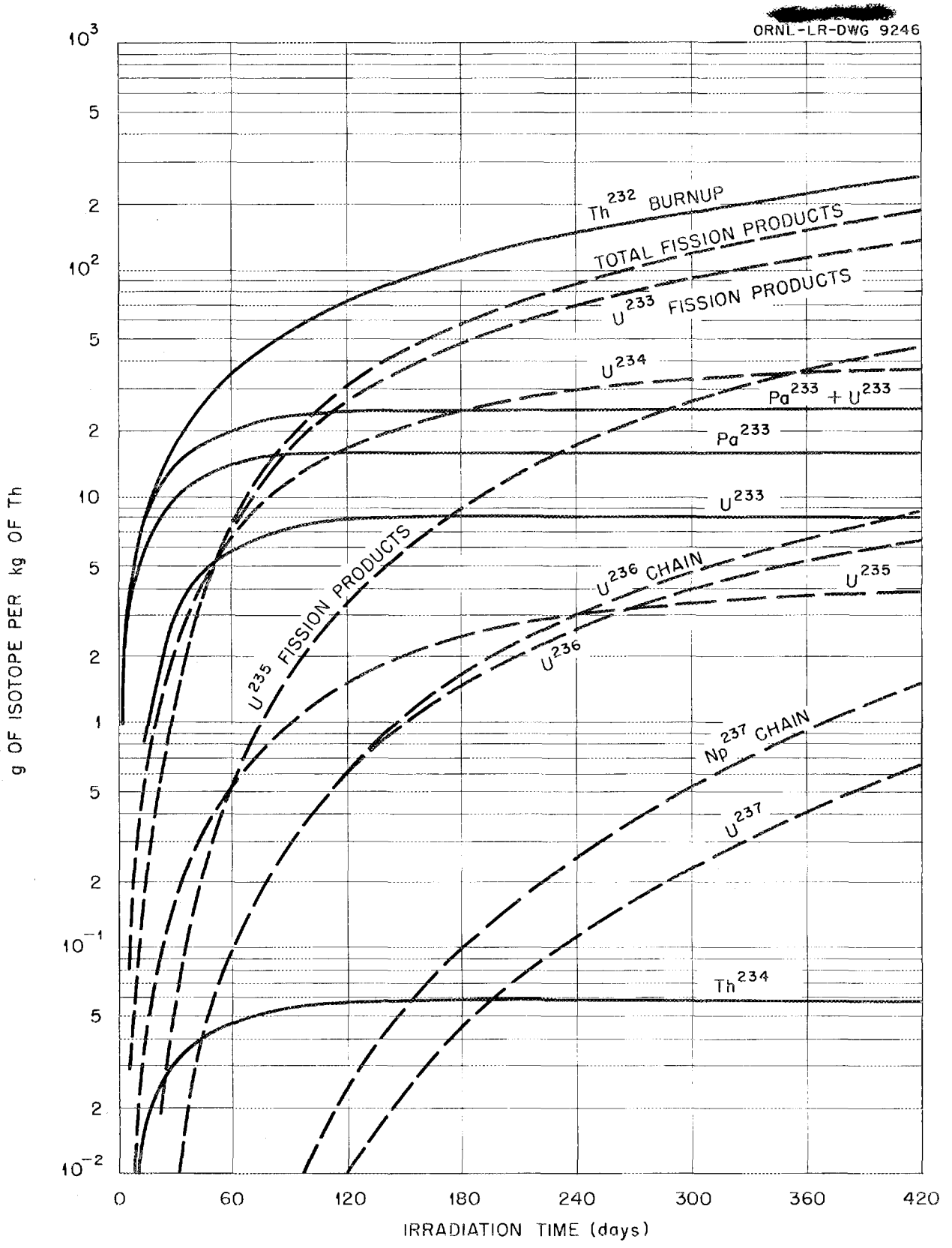

Fig. 8. Details of Products Produced by Neutron Irradiation (Long-Term) of Th^{232} at Flux of 10^{15} neutrons/cm^2·sec.

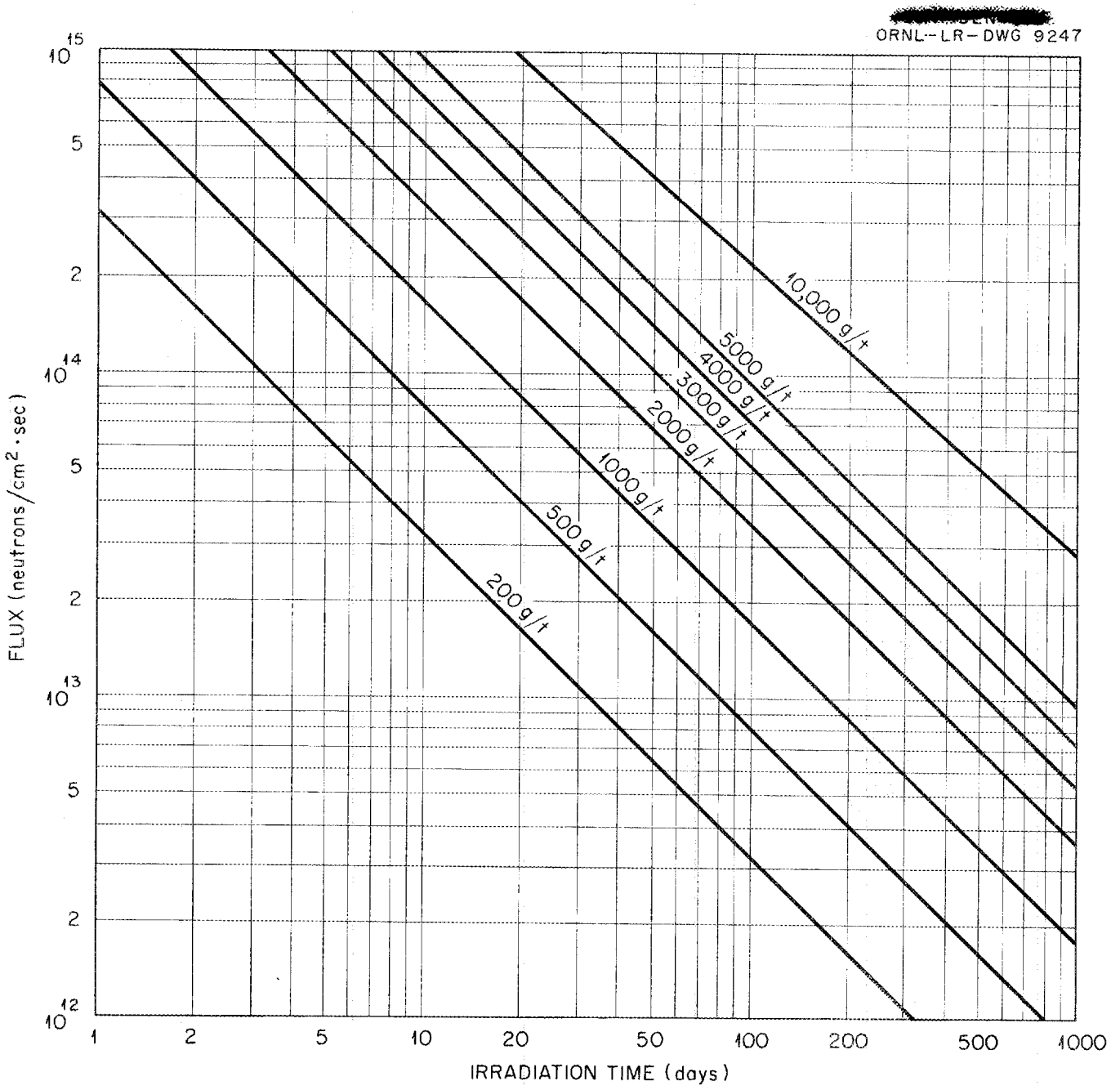

Fig. 9. Effect of Flux and Irradiation Time on Production of Isotopes of Mass 233.

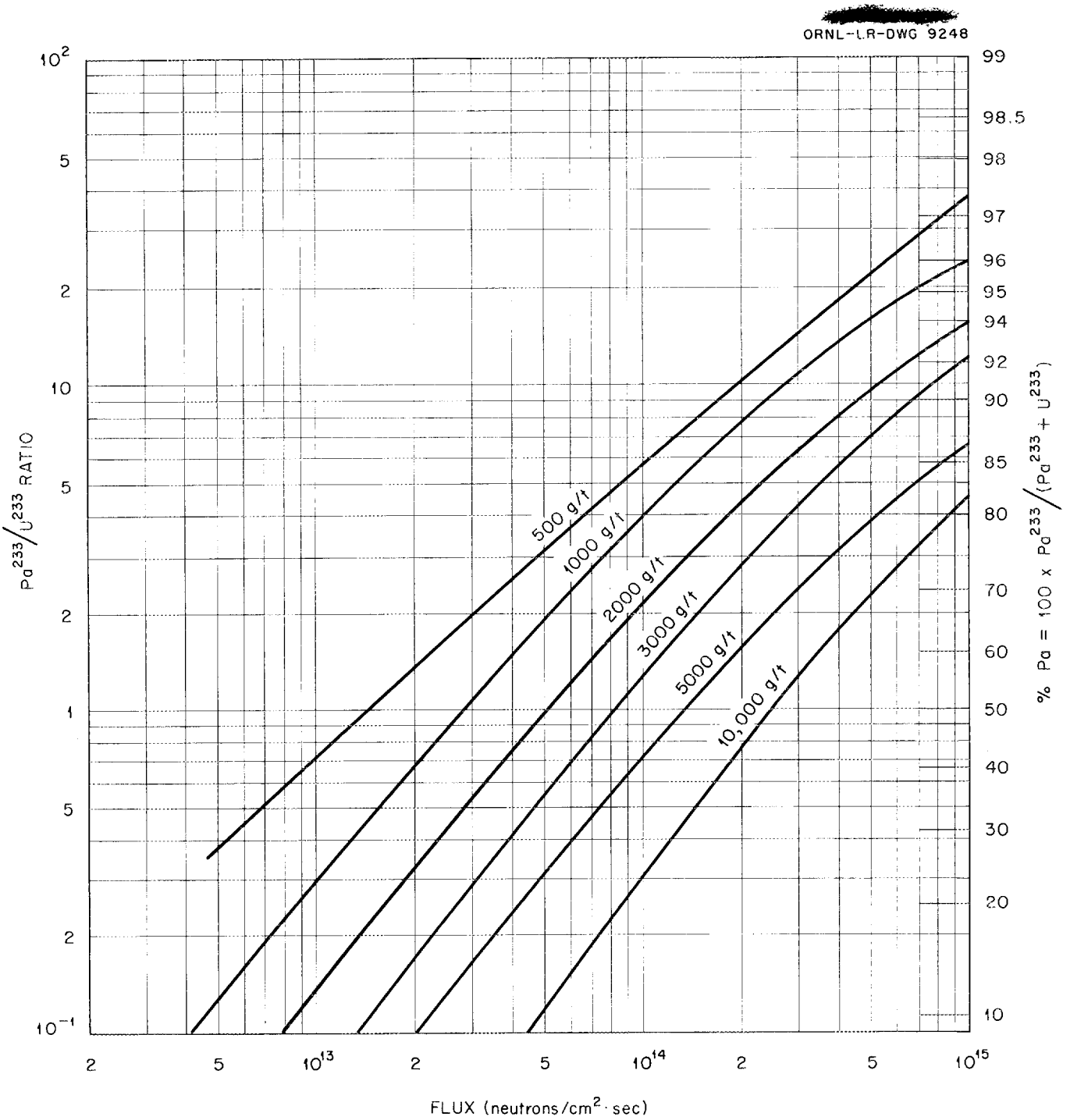

Fig. 10. Effect of Flux and Extent of Irradiation on Pa^{233}/U^{233} Ratio.

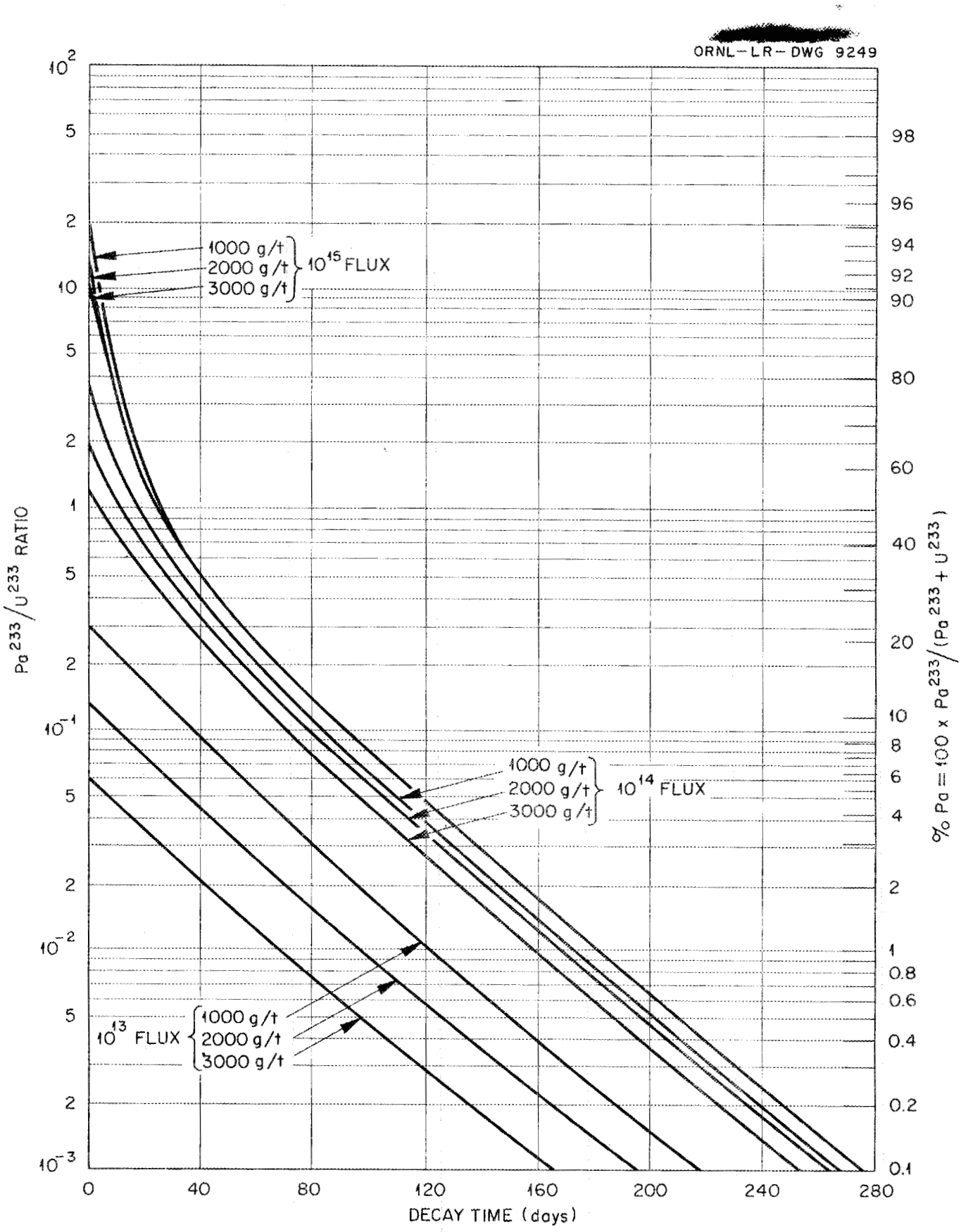

Fig. 11. Effect of Extent of Irradiation and Decay Time on Pa^{233}/U^{233} Ratio.

[redacted]

ORNL-LR-DWG 9308

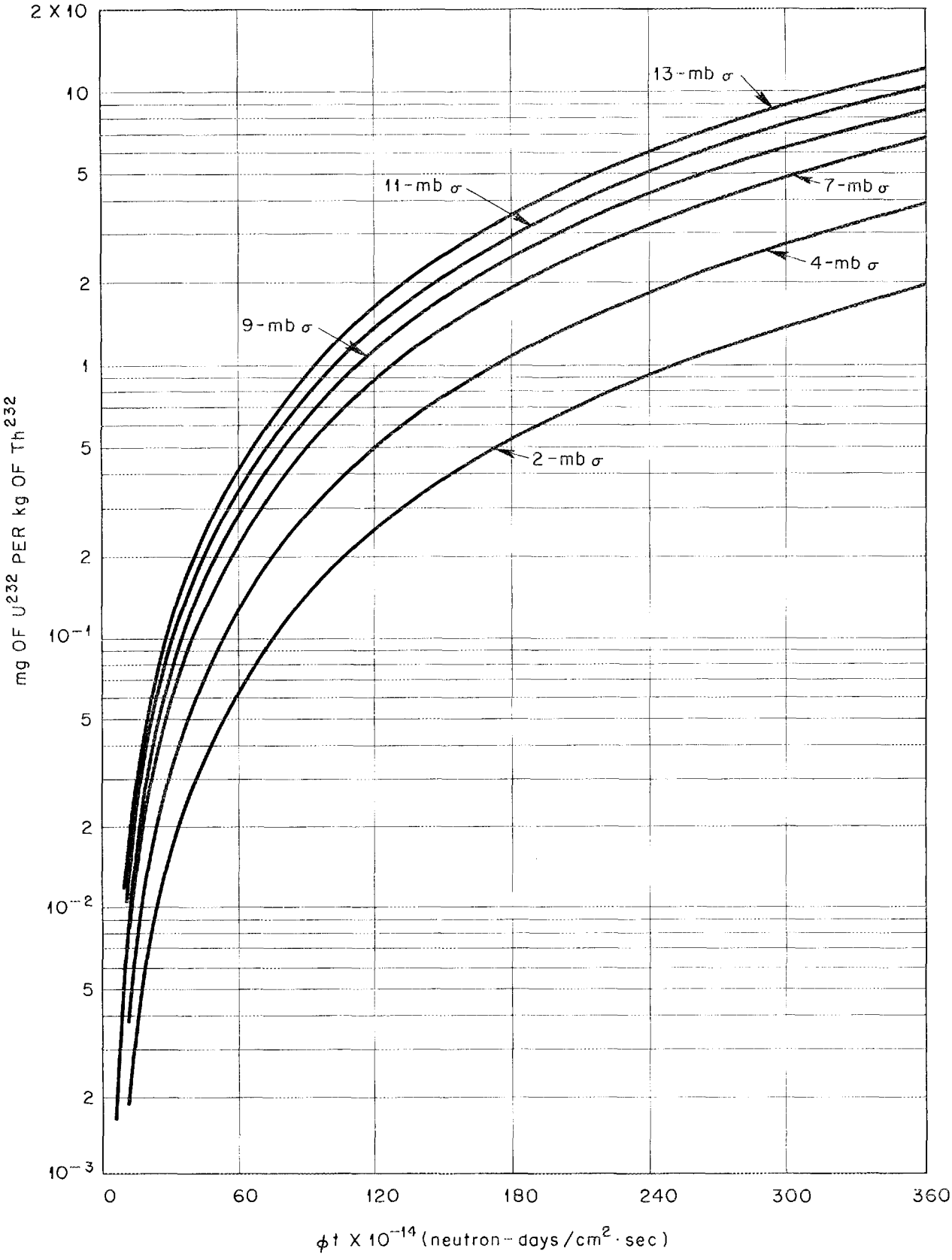

Fig. 12. Effect of Irradiation Time and Flux on Amount of U^{232} Formed.

Table 4. Effect of U^{232} Concentration on Total α Activity of Product as Total Mass 233

$\phi t \times 10^{-14}$ (n-days/cm^2/sec)	$U^{233} + Pa^{233}$ (g)	U^{233} Disintegration (g/y)	U^{232} at 2 mb Cross Section (g)	U^{232} Disintegration (g/y) [a]	U^{232}/U^{233} α Activity Ratio $\frac{U^{232}\text{ Disintegration}}{U^{233}\text{ Disintegration}}$
5	0.306	1.31×10^{-6}	4.66×10^{-7}	4.62×10^{-9}	3.53×10^{-3}
10	0.608	2.6×10^{-6}	1.865×10^{-6}	1.855×10^{-8}	7.15×10^{-3}
20	1.203	5.14×10^{-6}	7.46×10^{-6}	7.40×10^{-8}	1.44×10^{-2}
30	1.805	7.7×10^{-6}	1.68×10^{-5}	1.66×10^{-7}	2.16×10^{-2}
40	2.33	9.97×10^{-6}	3.04×10^{-5}	3.0×10^{-7}	3.01×10^{-2}
50	2.82	1.20×10^{-5}	4.46×10^{-5}	4.41×10^{-7}	3.68×10^{-2}
60	3.25	1.392×10^{-5}	6.30×10^{-5}	6.25×10^{-7}	4.49×10^{-2}
70	4.04	1.73×10^{-5}	8.74×10^{-5}	8.65×10^{-7}	5.0×10^{-2}
100	5.57	2.38×10^{-5}	1.745×10^{-4}	1.725×10^{-6}	7.26×10^{-2}
250	12.15	5.19×10^{-5}	9.4×10^{-4}	9.3×10^{-6}	1.79×10^{-1}
500	18.75	8.0×10^{-5}	3.35×10^{-3}	3.32×10^{-5}	4.15×10^{-1}
750	21.88	9.35×10^{-5}	6.53×10^{-3}	6.47×10^{-5}	6.92×10^{-1}
1000	23.18	9.98×10^{-5}	10.2×10^{-3}	10.1×10^{-5}	1.01

[a] The α activities listed are for U^{232} alone and do not include the daughter activities.

[redacted]
ORNL-LR-DWG 9309

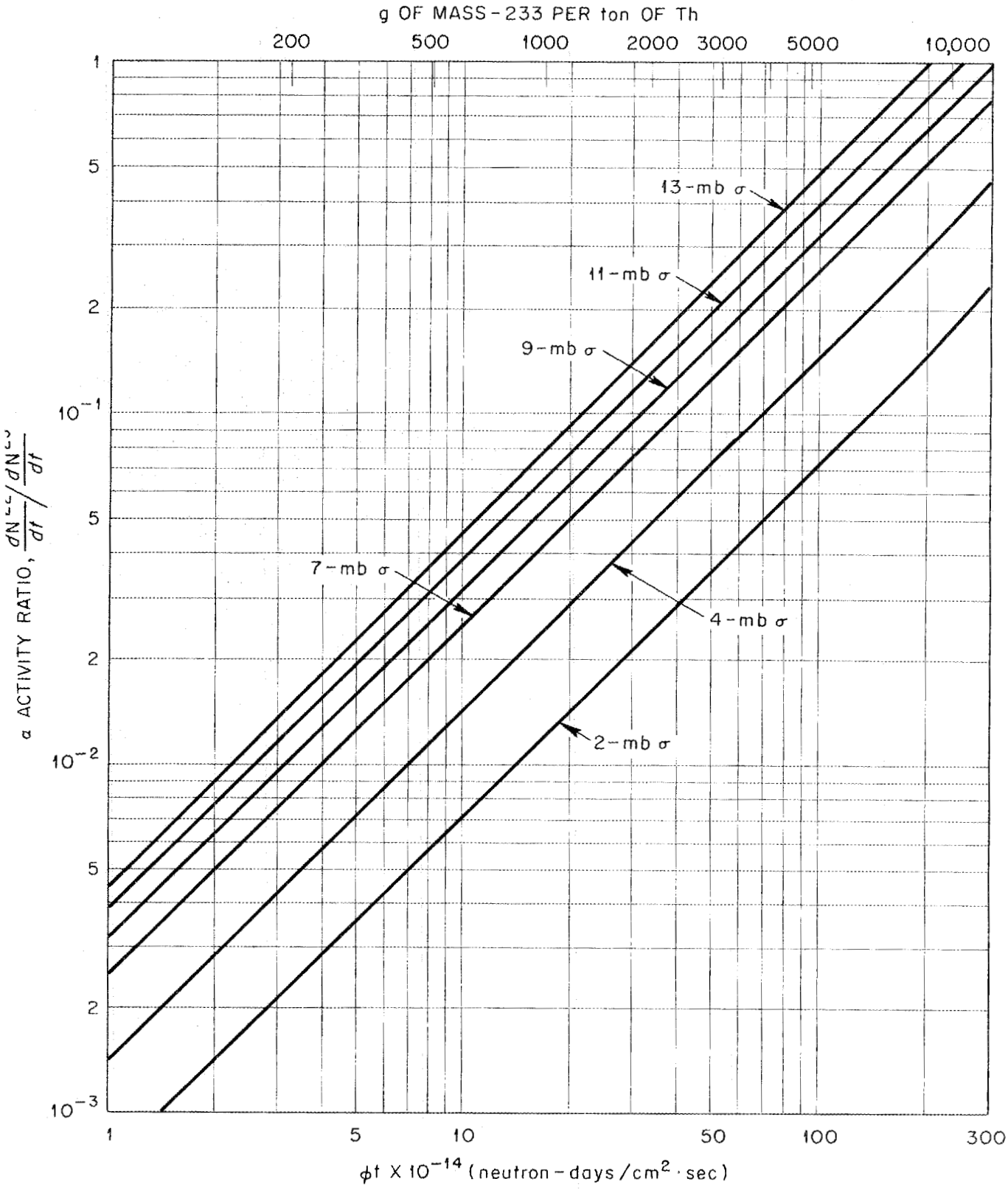

Fig. 13. Effect of Irradiation Time and Flux on U^{232}/U^{233} α Activity Ratio at Time of Discharge.

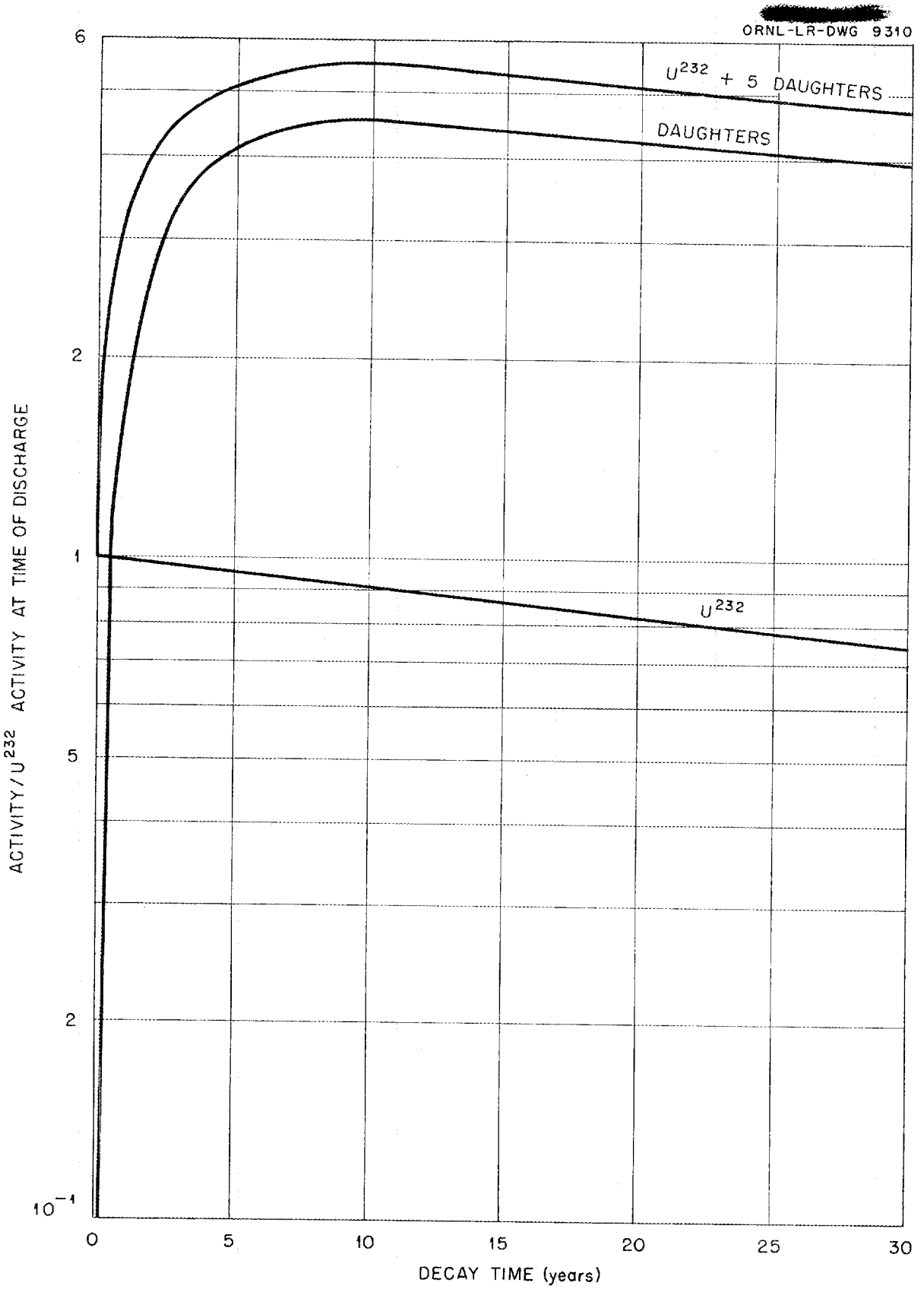

Fig. 14. Effect of Decay Time on U^{232} and Daughter Activities.

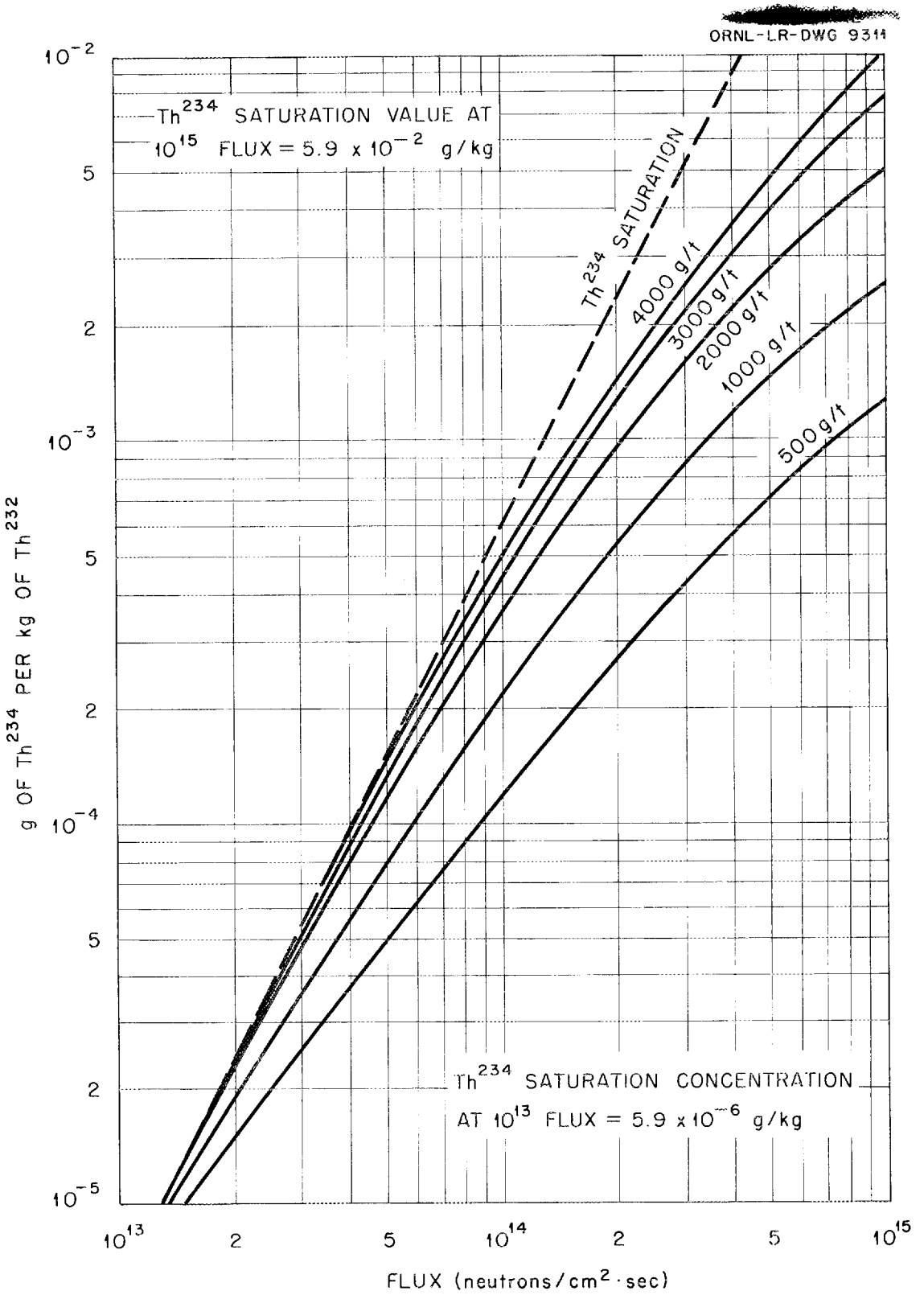

Fig. 15. Effect of Flux on Amount of Th^{234} Formed.

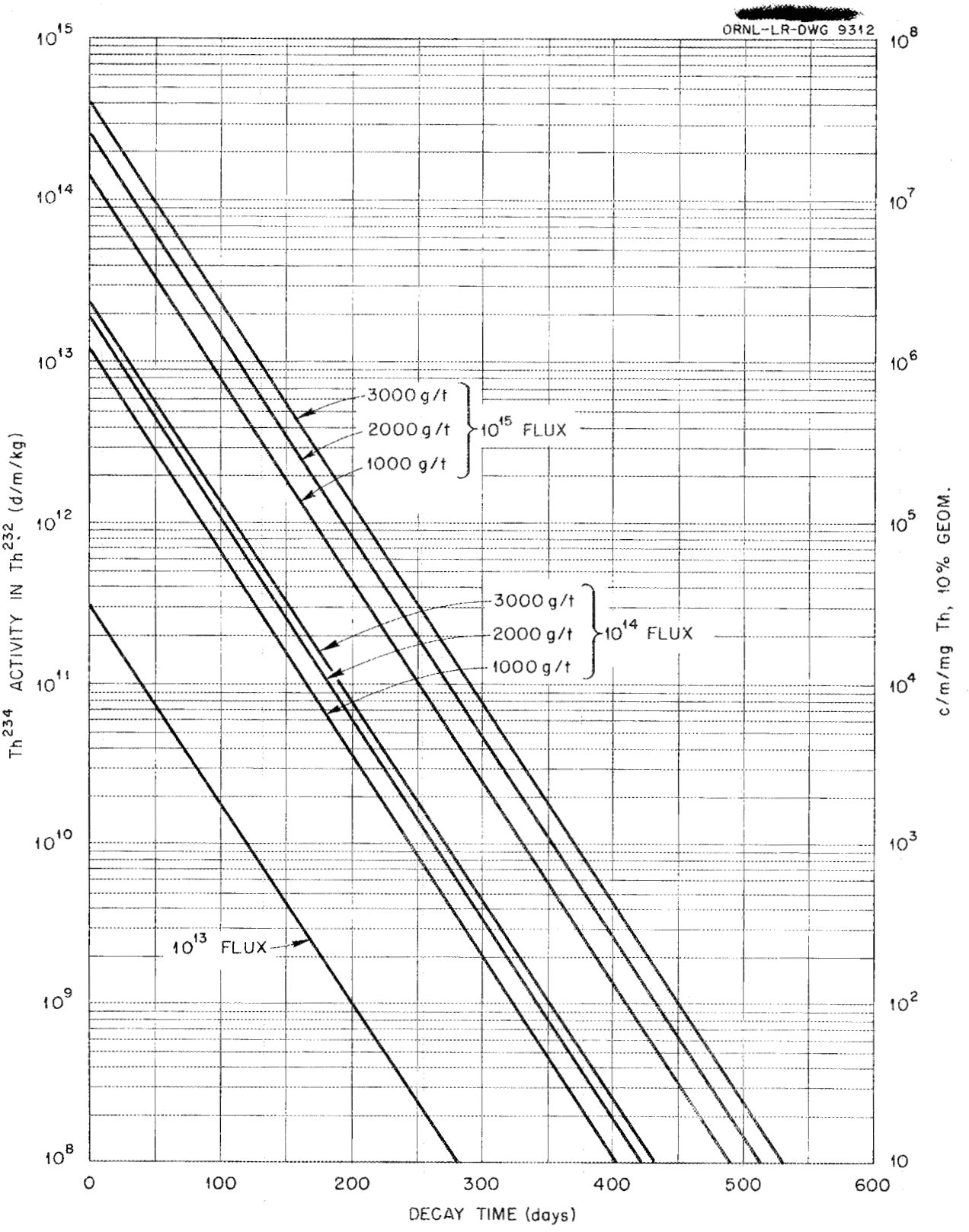

Fig. 16. Th^{234} Activity in Th^{232} as a Function of g/t Level, Flux, and Decay Time After Discharge.

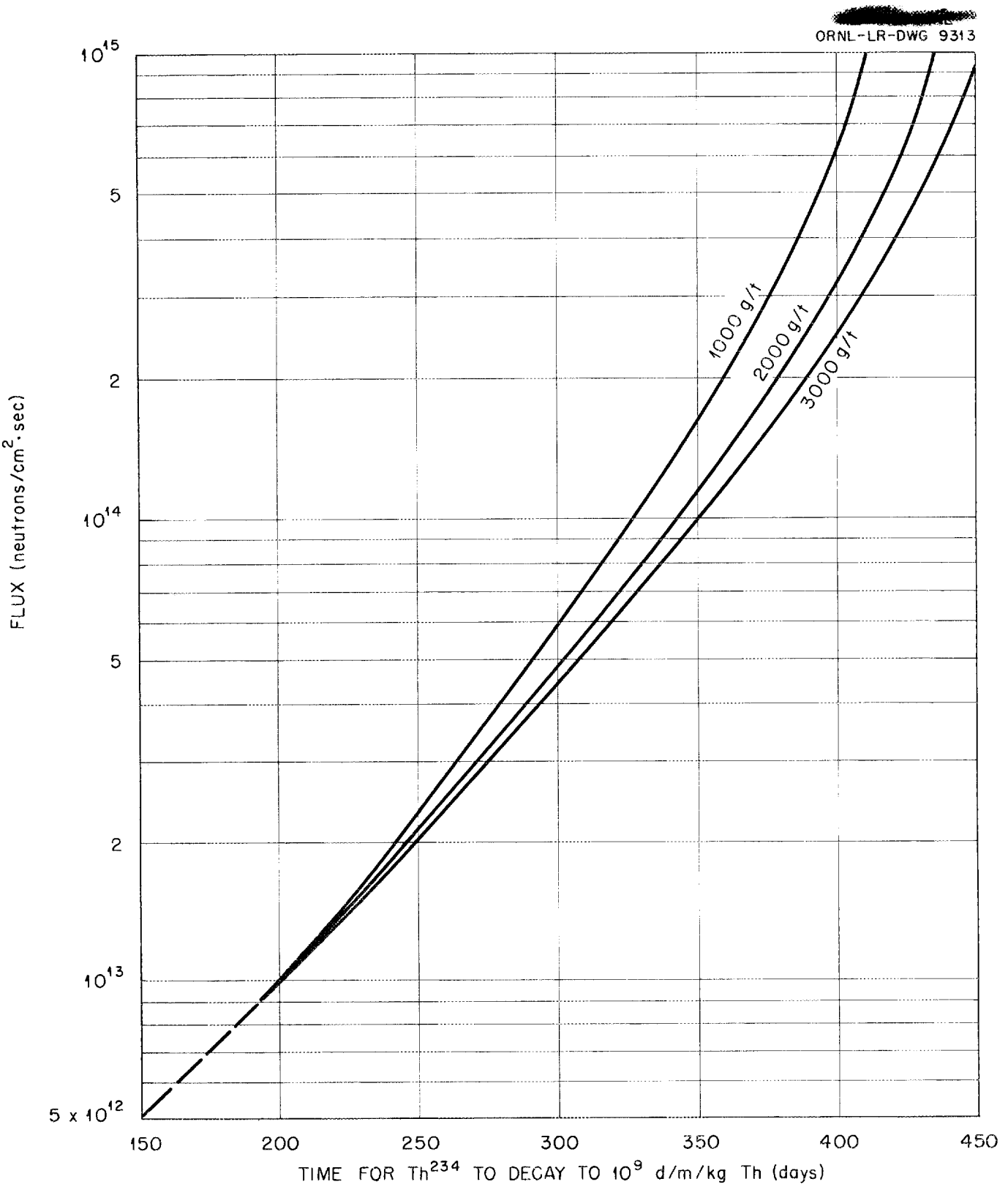

Fig. 17. Effect of Flux and g/t Level on Time Required After Discharge for Th^{234} to Decay to 10^9 d/m/kg.

Table 5. Concentrations and Activities of Ru^{103} and Ru^{106} at Time of Discharge[a]

Flux ($n/cm^2/sec$)	g/t Level (g mass 23/ton Th)	Irradiation Time (days)	Ru^{103}		Ru^{106}	
			Concentration (atoms/kg Th)	Activity (d/m/kg Th)	Concentration (atoms/kg Th)	Activity (d/m/kg Th)
10^{15}	1000	1.65	1.69×10^{16}	2.03×10^{11}	4.28×10^{15}	7.1×10^{9}
	2000	3.25	1.69×10^{17}	2.03×10^{12}	4.28×10^{16}	7.1×10^{10}
	3000	5	6.30×10^{17}	7.55×10^{12}	1.66×10^{17}	2.76×10^{11}
10^{14}	1000	17	2.94×10^{17}	3.53×10^{12}	8.56×10^{16}	1.42×10^{11}
	2000	34	7.85×10^{17}	9.41×10^{12}	2.64×10^{17}	4.38×10^{11}
	3000	53	1.74×10^{18}	2.09×10^{13}	6.34×10^{17}	1.05×10^{12}
10^{13}	1000	175	1.37×10^{17}	1.64×10^{12}	9.0×10^{16}	1.49×10^{11}
	2000	355	4.72×10^{17}	5.66×10^{12}	4.95×10^{17}	8.21×10^{11}
	3000	540	8.25×10^{17}	9.9×10^{12}	1.1×10^{18}	1.83×10^{12}

[a] Yield of Ru^{103} = 0.93%; yield of Ru^{106} = 0.235%.

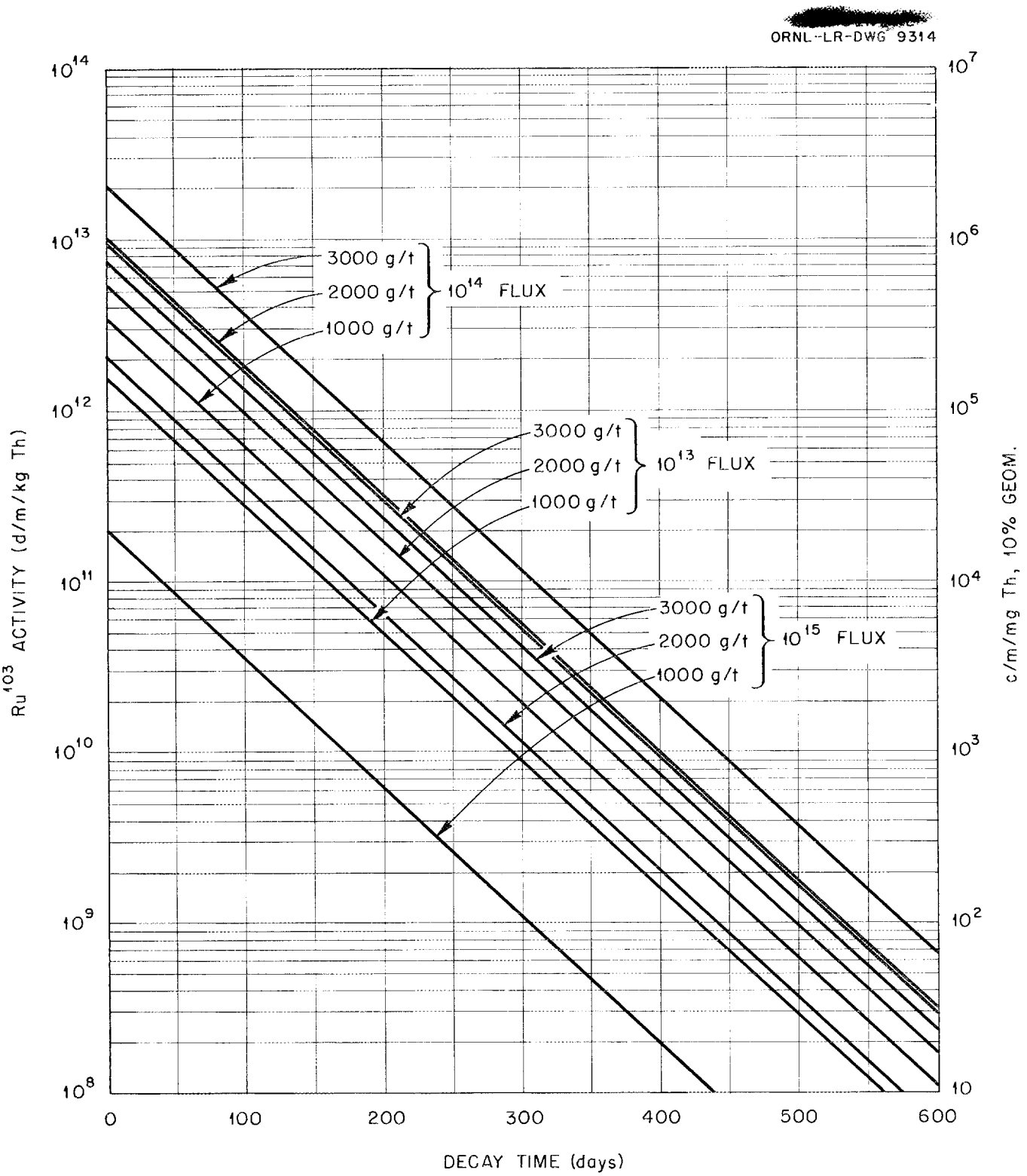

Fig. 18. Effect of Flux, g/t Level, and Decay Time After Discharge on Ru^{103} Activity.

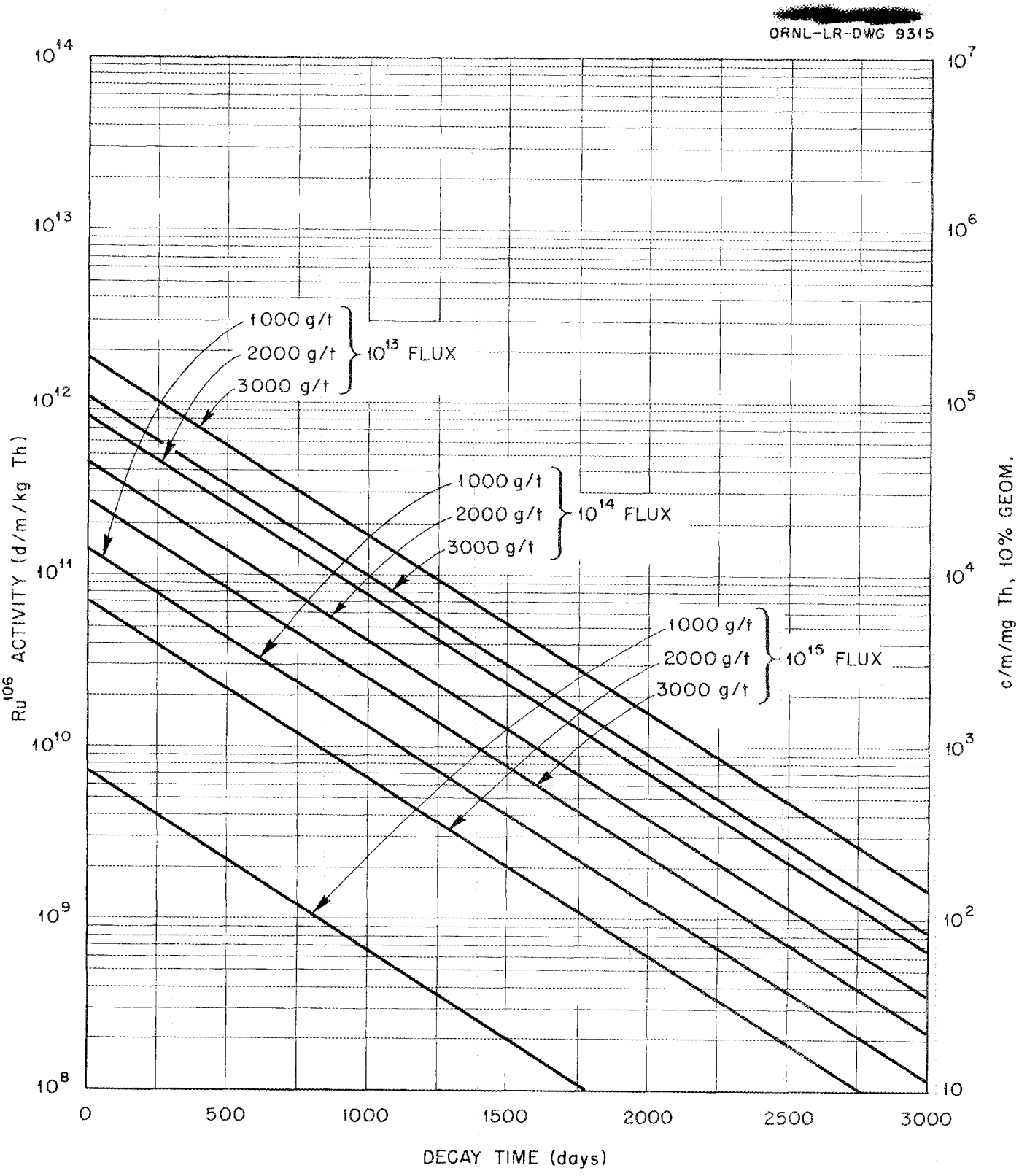

Fig. 19. Effect of Flux, g/t Level, and Decay Time After Discharge on Ru^{106} Activity.

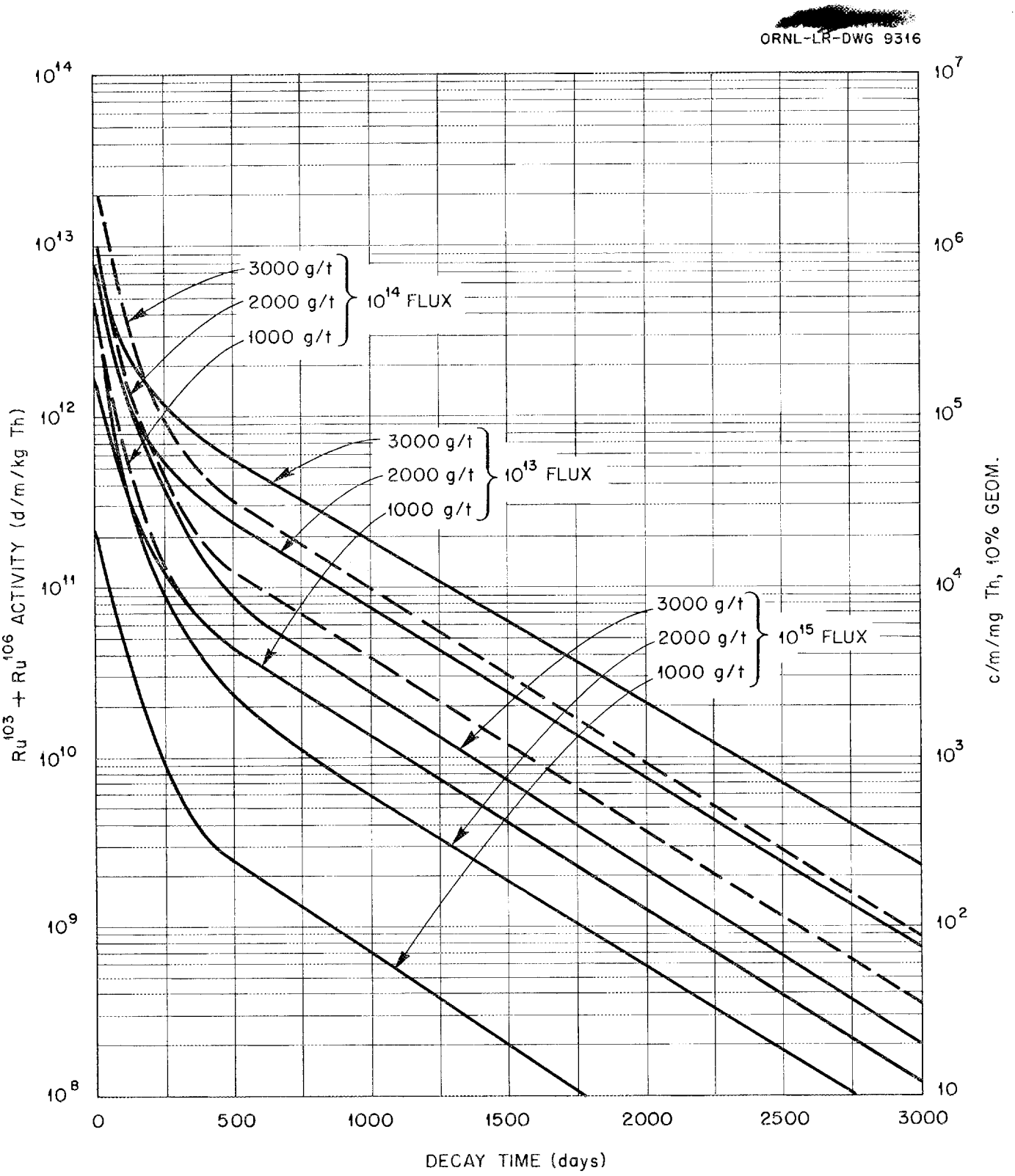

Fig. 20. Effect of Flux, g/t Level, and Decay Time After Discharge on $Ru^{103} + Ru^{106}$ Activity.

The concentrations and activities listed in Table 4 were obtained by using a 2-mb cross section for the (n,2n) reaction. The concentrations and activities for other cross sections are simple multiples of those obtained for 2 mb.

Equations* used to calculate U^{232} concentration and activity. The differential equations involved in the formation of U^{232} are

$$\frac{dN_{22}}{dt} = N_{11}\phi\,\sigma_{11} \qquad (1)$$

and

$$\frac{dN_{11}}{dt} = \phi N_{02}\sigma_{02} - N_{11}\phi\,\sigma_{11} \qquad (2)$$

These equations are integrated to give

$$N_{11} = \frac{\phi N_{02}\sigma_{02}}{\phi\,\sigma_{11}}\left(1 - e^{-\phi\,\sigma_{11}t}\right) \qquad (3)$$

and

$$N_{22} = N_{02}\sigma_{02}\left[\phi t - \frac{1}{\sigma_{11}}\left(1 - e^{-\phi\,\sigma_{11}t}\right)\right] \qquad (4)$$

In order to compare U^{233} products produced at different g/t levels or by decay of isolated Pa^{233}, it is necessary to determine the α activity due to U^{232}. This is done by determining the α activity ratio:

$$\alpha \text{ activity ratio} = \left(\frac{dN_{22}}{dt}\right)\Big/\left(\frac{dN_{23}}{dt}\right) = \frac{N_{22}\,\lambda_{22}}{N_{23}\,\lambda_{23}}$$

U^{232} decays to a series of α-emitting daughters (Table 6) with a half-life of 1.9y, the half-life of Th^{228}. Hence in 1.9y the daughter α activities are equal to half their equilibrium value. After 10 years the total α activity reaches a maximum of 5.2 times the U^{232} activity at time of reactor discharge, or 5.7 times the U^{232} activity then present.

* See Sec. 6.0 for definition of symbols and numerical values of constants.

With $N^{o}_{08} = 0$ and neglecting the half-lives of the remainder of the series, the equation for the activity, A_s, of the daughter series as a function of decay time after discharge becomes

$$A_s = 5A^{o}_{22} \frac{\lambda_{08}}{\lambda_{22} - \lambda_{08}} \left(e^{-\lambda_{22}t} - e^{-\lambda_{08}t}\right)$$

Table 6. Daughters of U^{232}

Nuclide	Half-life	α (Mev)	% Decay by α Emission
U^{232}	70y	5.31	100
Th^{228}	1.9y	5.40	100
Ra^{224}	3.64d	5.68	100
Rn^{220}	55s	6.28	100
Po^{216}	0.16s	6.77	100
Pb^{212}	10.6h	---	0
$Bi^{212}(\alpha,\beta)$	60m	6.08	34
Po^{212} [a]	10^{-6}s	8.78	100

[a] Only 66% of Pb^{212} formed in the chain reaches Po^{212}.

5.0 CALCULATIONS

In all cases the exact solution to a given differential equation was used except for those low values of ϕt in which the approximate equation was found to be accurate to within 1 percent. In many cases in which the solution was very complex, the approximate equation was more accurate for short irradiation times since the exact solution usually involved subtraction of two numbers of approximately the same magnitude.

All calculations were based on the cross section and half-life values listed in Sec. 6.0. The cross section values given are those for thermal neutrons at room temperature. The curves thus obtained apply only to those conditions and would give only approximate answers at other temperatures for which there are different cross section values. To obtain more exact

answers at other conditions, the equations should be solved with the corrected cross-section values. In some cases it can be seen that the standard 1/velocity correction factor could be applied to the cross sections without affecting more than one term of an equation. If this is the case, concentrations at different temperature conditions could easily be obtained from the graphs with only minor calculations. However, for most cases, the terms that are affected by cross-section changes are exponentials or factors involving both $\phi\ \sigma$ and λ terms. In these cases it probably would be easier to solve the equation with the corrected cross-section value.

In this study thermal flux and thermal cross sections were used, and no correction for resonance was made since resonance absorption varies with the type of reactor. The term $\overline{\phi\ \sigma_{02}}$ is given in the equations as a correction factor applied to ϕ to include resonance absorption in Th^{232} and should be used where greater accuracy is desired.

All calculations were based upon 1 kg of thorium, and the amount of thorium was assumed to be a constant during the entire irradiation period. The following equations were used:

For thorium burnup,

$$\frac{dN'_{02}}{dt} = N_{02}\overline{\phi\ \sigma_{02}} \tag{1}$$

$$N'_{02} = N_{02}\overline{\phi\ \sigma_{02}}t \tag{2}$$

For production of U^{233} and Pa^{233},

$$\frac{dN_{23}}{dt} = N_{13}\ \lambda_{13} - N_{23}\phi\sigma'_{23} \tag{3}$$

$$N_{23} = \frac{N_{02}\ \overline{\phi\ \sigma_{02}}\ \lambda_{13}}{\phi\sigma'_{23}(\lambda_{13} + \phi\ \sigma_{13} - \phi\ \sigma'_{23})(\lambda_{13} + \phi\ \sigma_{13})} \times \left[(\lambda_{13} + \phi\ \sigma_{13})(1-e^{-\phi\ \sigma'_{23}t}) - \phi\ \sigma'_{23}(1-e^{-(\lambda_{13} + \phi\ \sigma_{13})t})\right] \tag{4}$$

$$\frac{dN_{13}}{dt} = N_{02}\,\overline{\phi\,\sigma_{02}} - \phi N_{13}\sigma_{13} - \lambda_{13}N_{13} \tag{5}$$

$$N_{13} = \frac{N_{02}\overline{\phi\,\sigma_{02}}}{\lambda_{13} + \phi\,\sigma_{13}}\left[1-e^{-(\lambda_{13} + \phi\,\sigma_{13})t}\right] \tag{6}$$

For production of U^{234}, assuming that this isotope was produced by both capture of a neutron by U^{233} and capture of a neutron by Pa^{233} followed by decay of the Pa^{234} to U^{234},

$$\frac{dN_{24}}{dt} = N_{23}\phi\,\sigma_{23} + N_{13}\phi\,\sigma_{13} - N_{24}\phi\,\sigma_{24} \tag{7}$$

$$N_{24} = A\left\{B\left[\phi\,\sigma_{24}(1-e^{-\phi\,\sigma'_{23}t}) - \phi\,\sigma'_{23}(1-e^{-\phi\,\sigma_{24}t})\right] + C\left[(\lambda_{13} + \phi\,\sigma_{13})(1-e^{-\phi\,\sigma_{24}t}) - \phi\,\sigma_{24}(1-e^{-(\lambda_{13} + \phi\,\sigma_{13})t})\right]\right\} \tag{8}$$

where
$$A = \frac{N_{02}\overline{\phi\,\sigma_{02}}}{(\lambda_{13} + \phi\,\sigma_{13} - \phi\,\sigma'_{23})(\lambda_{13} + \phi\,\sigma_{13})}$$

$$B = \frac{\lambda_{13}\sigma_{23}}{\sigma'_{23}}\,\frac{\lambda_{13} + \phi\,\sigma_{13}}{\phi\,\sigma_{24}(\phi\,\sigma_{24} - \phi\,\sigma'_{23})}$$

$$C = \frac{(\lambda_{13} + \phi\,\sigma_{13} - \phi\,\sigma'_{23})\,\sigma_{13} - \lambda_{13}\sigma_{23}}{\sigma_{24}(\lambda_{13} + \phi\,\sigma_{13} - \phi\,\sigma_{24})}$$

For production of fission products from U^{233},

$$\frac{dN_{FP}}{dt} = 2\phi N_{23}\sigma_{f23} \tag{9}$$

$$N_{FP} = \frac{2N_{02}\overline{\phi\,\sigma_{02}}\lambda_{13}\sigma_{f23}}{\sigma'_{23}(\lambda_{13} + \phi\,\sigma_{13} - \phi\,\sigma'_{23})(\lambda_{13} + \phi\,\sigma_{13})}\left\{\frac{\lambda_{13} + \phi\,\sigma_{13}}{\phi\,\sigma'_{23}} \times \left[\phi\,\sigma'_{23}t-(1-e^{-\phi\,\sigma'_{23}t})\right] - \frac{\phi\,\sigma'_{23}}{\lambda_{13} + \phi\,\sigma_{13}}\left[(\lambda_{13} + \phi\,\sigma_{13})t - (1-e^{-(\lambda_{13} + \phi\sigma_{13})t}\right]\right\} \tag{10}$$

For formation of Th^{234},

$$\frac{dN_{04}}{dt} = N_{03}\phi\,\sigma_{03} - N_{04}\,\lambda_{04} \tag{11}$$

$$N_{04} = \frac{N_{02}\,\overline{\phi\,\sigma_{02}}\,\phi\,\sigma_{03}}{\lambda_{04}(\lambda_{03} + \phi\,\sigma_{03} - \lambda_{04})(\lambda_{03} + \phi\,\sigma_{03})} \times \left[(\lambda_{03} + \phi\,\sigma_{03})(1-e^{-\lambda_{04}t}) - \lambda_{04}(1-e^{-(\lambda_{03} + \phi\sigma_{03})t}\right] \tag{12}$$

Since λ_{03} is much larger than $\phi\sigma_{03}$ or λ_{04}, the approximate form was used,

$$N_{04} = \frac{N_{02}\overline{\phi\,\sigma_{02}}\,\phi\,\sigma_{03}}{\lambda_{04}\,\lambda_{03}^{2}}\left[\lambda_{03}(1-e^{-\lambda_{04}t}) - \lambda_{04}\right] \tag{13}$$

$$\frac{dN_{03}}{dt} = N_{02}\,\overline{\phi\,\sigma_{02}} - N_{03}\,\lambda_{03} - N_{03}\,\phi\,\sigma_{03} \tag{14}$$

$$N_{03} = \frac{N_{02}\,\overline{\phi\,\sigma_{02}}}{\lambda_{03} + \phi\,\sigma_{03}}\left[1-e^{-(\lambda_{03} + \phi\,\sigma_{03})t}\right] \tag{15}$$

For formation of U^{235},

$$\frac{dN_{25}}{dt} = N_{24}\,\phi\,\sigma_{24} - N_{25}\,\phi\,\sigma'_{25} \tag{16}$$

Substituting the expression for N_{24} previously calculated (Eq. 8) gives

$$N_{25} = \frac{A\,\sigma_{24}}{\sigma'_{25}}\left(B\left\{\frac{\phi\,\sigma_{24}}{\phi\,\sigma'_{25} - \phi\,\sigma'_{23}}\left[\phi\,\sigma'_{25}(1-e^{-\phi\,\sigma'_{23}t}) - \phi\,\sigma'_{23}(1-e^{-\phi\sigma'_{25}t})\right] - \frac{\phi\,\sigma'_{23}}{\phi\,\sigma'_{25} - \phi\,\sigma_{24}}\left[\phi\,\sigma'_{25}(1-e^{-\phi\,\sigma_{24}t}) - \phi\,\sigma_{24}(1-e^{-\phi\sigma'_{25}t})\right]\right\} + C\left\{\frac{\lambda_{13} + \phi\,\sigma_{13}}{\phi\,\sigma'_{25} - \phi\,\sigma_{24}} \times \left[\phi\,\sigma'_{25}(1-e^{-\phi\,\sigma_{24}t}) - \phi\,\sigma_{24}(1-e^{-\phi\,\sigma'_{25}t})\right] - \frac{\phi\,\sigma_{24}}{\lambda_{13} + \phi\,\sigma_{13} - \phi\,\sigma'_{25}} \times \left[(\lambda_{13} + \phi\,\sigma_{13})(1-e^{-\phi\,\sigma'_{25}t}) - \phi\,\sigma'_{25}(1-e^{-(\lambda_{13} + \phi\,\sigma_{13})t})\right]\right\}\right) \tag{17}$$

where
$$A = \frac{N_{02}\,\overline{\phi\,\sigma_{02}}}{(\lambda_{13} + \phi\,\sigma_{13} - \phi\,\sigma'_{23})(\lambda_{13} + \phi\,\sigma_{13})}$$

$$B = \frac{\lambda_{13}\,\sigma_{23}}{\sigma'_{23}}\left(\frac{\lambda_{13} + \phi\,\sigma_{13}}{\phi\,\sigma_{24}(\phi\,\sigma_{24} - \phi\,\sigma'_{23})}\right)$$

$$C = \frac{(\lambda_{13} + \phi\,\sigma_{13} - \phi\,\sigma'_{23})\,\sigma_{13} - \lambda_{13}\,\sigma_{23}}{\sigma_{24}\,(\lambda_{13} + \phi\,\sigma_{13} - \phi\,\sigma_{24})}$$

For formation of fission products from U^{235}, calculations were made by using the U^{235} curve over successive 30-day increments, according to the scheme

$$\frac{dN_{FP}}{dt} = N_{25}\,\phi\,\sigma_{f25} \tag{18}$$

$$N_{FP} = \phi\,\sigma_{f25}\int_0^t N_{25}\,dt \tag{19}$$

$$N_{FP} \doteq \phi\,\sigma_{f25}\sum_{i=0}^{t} N_{i25}\,\Delta t_i \tag{20}$$

where N_{i25} is the average U^{235} concentration during time interval Δt_i.

Schemes similar to the above were used to calculate the formation of U^{236}, U^{237}, and Np^{237}. U^{236} chain quantities were obtained in a manner similar to that used for fission products except that the U^{235} capture cross section was used. U^{237} and Np^{237} formations were then calculated from the U^{236} chain quantities. There are more inaccuracies in the U^{237} and Np^{237} calculations than in those for U^{236} and fission products. The curves for U^{237} and Np^{237} are probably within 10% of the analytical value.

For Th^{234} decay, the activity was determined from the Th^{234} concentration corresponding to the various g/t levels. The cooling period was decided as that period required for Th^{234} activity to decay to 10^9 d/m/kg Th, or 100 c/m/mg at 10% geometry.

For Ru^{106} and Ru^{103} activities, calculations were made from the fission product concentration curves by using the respective yields and integrating with respect to the decay function. The buildup is given by

$$N_{Ru} = \frac{N_{FP}y}{2} \frac{1}{T} \int_0^t e^{-\lambda t} dt = \frac{N_{FP}y}{2} \left[\frac{(1-e^{-\lambda T})}{\lambda T} \right] \tag{21}$$

The decay rate at the time of reactor discharge is given by

$$\frac{dN_{Ru}}{dt} = -N_{Ru}\lambda = \frac{-N_{FP}y}{2} \left[\frac{(1-e^{-\lambda T})}{\lambda T} \right] \lambda \tag{22}$$

6.0 CONSTANTS AND DEFINITION OF SYMBOLS

The following symbols are used in this report:

ϕ = flux ($n/cm^2/sec$)

t = time (sec)

N = atoms of given nuclide formed

N^o = atoms of given nuclide present initially

N' = atoms of given nuclide burned up

y = fission yield of given fission product

T = time of irradiation used to find extent of fission product decay

A^o = activity at time of reactor discharge

02 = Th^{232}

11 = Pa^{231}

13 = Pa^{233}

22 = U^{232}

23 = U^{233}

24 = U^{234}

25 = U^{235}

26 = U^{236}

27 = U^{237}

FP = fission products

Table 7. Cross-section Values

Symbol	Value (barns)	Symbol	Value (barns)
Capture		Absorption	
σ_{02}	7	σ'_{23}	560
σ_{03}	1350	σ'_{25}	640
σ_{11}	250	Fission	
σ_{13}	150	σ_{f23}	505
σ_{23}	55	σ_{f25}	540
σ_{24}	70	Reaction	
σ_{25}	100	$\sigma_{02}(n,2n)$	0.002-0.013
σ_{26}	20		

Table 8. Half-life Values

Nuclide	Type of Emission and Energy (Mev)	Half-life
Th^{231}	β^- 0.3,0.22,0.09; γ 0.022-0.21	25.5h
Th^{232}	α 4.03	1.39×10^{10}y
Th^{233}	β^- 1.23	23.5m
Th^{234}	β^- 0.2, 0.11; γ 0.093	24.1d
Pa^{232}	β^- 0.33; γ 0.05 - 0.96	1.32d
Pa^{233}	β^- 0.58,0.48,0.27; γ 0.1, 0.31	27.4d
Pa^{234} [a]	β^- 2.3; γ 0.8	1.14m
U^{232}	α 5.31	70y
U^{233}	α 4.82	1.62×10^5y
U^{234}	α 4.76	2.6×10^5y
U^{235}	α 4.2 - 4.6	7.1×10^8y
U^{237}	β^- 0.23; γ 0.2, 0.06, 0.26	6.7d
Ru^{103}	β^- 0.217; γ 0.498	40d
Ru^{106}	β^- 0.038	290d

[a] Pa^{234} as UZ with a 6.7h half-life was not considered. The Pa^{234} was assumed to be UX_2 whether formed by Th^{234} decay or a $Pa^{233}(n,\gamma)$ reaction.

Table 9. Decay Constant Values

Symbol	Value
λ_{08}	$3.647 \times 10^{-1} y^{-1}$
λ_{22}	$9.9 \times 10^{-3} y^{-1}$
λ_{23}	$4.28 \times 10^{-6} y^{-1}$
$\lambda_{Ru^{103}}$	$1.2 \times 10^{-5} m^{-1}$
$\lambda_{Ru^{106}}$	$1.66 \times 10^{-6} m^{-1}$

7.0 REFERENCES

1. E. D. Arnold and A. T. Gresky, ORNL-1817 (in press)
2. R. W. Stoughton, D. E. Ferguson, J. Halperin, and C. V. Ellison, ORNL-1462 (May 5, 1953)
3. P. Fields, E. Gerngross, and H. Diamond, ANL-4861 (February 1, 1952)
4. E. K. Hyde, R. J. Bruehlman, and W. M. Manning, ANL-4165 (June 25, 1948)
5. L. I. Katzin, CB-3767 (March 25, 1947)
6. R. W. Stoughton and J. Halperin, ORNL, letter to F. L. Culler, ORNL (January, 1954)